Chapter V

Aggregation number of dodecyl benzene sulfonate micelles with varying counterion and the interaction with oxazine dye in aqueous media: a fluorescence spectroscopic study

Chapter V

Aggregation number of dodecyl benzene sulfonate micelles with varying counterion and the interaction with oxazine dye in aqueous medium: a fluorescence spectroscopic study

5. 1 Introduction

During the past two decades there has been a remarkable growth in the use of fluorescence in the biological sciences. Fluorescence is now used in environmental monitoring, clinical chemistry, DNA sequencing, and genetic analysis by fluorescence *in situ* hybridization (FISH). Because of the sensitivity of fluorescence detection, and the expense and difficulties of handling radioactive substances, there is a continuing development of medical tests based on the phenomenon of fluorescence. These tests include the widely used enzyme-linked immunoassays (ELISA) and fluorescence polarization immunoassays.

Luminescence is the emission of light from any substance and occurs from electronically excited states. Luminescence is formally divided into two categories, fluorescence and phosphorescence, depending on the nature of the excited state. In the singlet states, the electron in the excited orbital is paired (of opposite spin) to the second electron in the ground-state orbital. Consequently, return to the ground state is spin-allowed and occurs rapidly by emission of a photon. The emission rates of fluorescence are typically 10^8 s^{-1}, so that a typical fluorescence lifetime is near 10 ns. Phosphorescence is emission of light from triplet excited states, in which the electron in the excited orbital has the same spin orientation as the ground state electron. Transition to the ground state are forbidden and the emission rates are slow (10^3 – 10^0 s^{-1}). Fluorescence typically occurs from aromatic molecules. Some typical fluorescent substances (fluorophores) are quinine, fluorescein, rhodamine B etc. The first observation of fluorescence from a quinine solution in sunlight was reported by Sir John Frederick William Herschel in 1845 [1].

Within the next decade, one can anticipate the introduction of numerous point-of-care fluorescence assays for use at the bedside, in the doctor's office, or for home

health care. The essence of any experiment is the existence of an observable quantity and the correlation of the value of this observable with a phenomenon of interest. The time span between the absorption of light and its subsequent reemission allows time for several processes, each of which results in changes of fluorescence spectral observables. These processes include collisions with quencher, as discussed in this chapter, rotational and translational diffusion, formation of complexes with solvents or solutes, and reorientation of the environment surrounding the altered dipole moment of the excited state. These dynamic processes can affect the fluorescence anisotropies, quantum yields, lifetimes, and emission spectra. In addition, resonance energy transfer provides a reliable indicator of molecular proximity on the angstrom size scale. As a result, the spectral characteristics of fluorophores can provide a great deal of information on the solution behaviour of macromolecules.

5.2. Steady State Fluorescence

Fluorescence spectral data are generally presented as emission spectra. A fluorescence emission spectrum is a plot of the fluorescence intensity versus wave length (nanometers) or wave number (cm^{-1}). The processes which occur between the absorption and emission of light are usually illustrated by a Jabłoński diagram. The fluorescence lifetime and quantum yield are perhaps the most important characteristics of a fluorophore. The quantum yield is the number of emitted photons relative to the number of absorbed photons. Substances with the largest quantum yields, approaching unity, such as rhodamine, display the brightest emission. The lifetime is also important, as the lifetime determines the time available for the fluorophore to interact with or diffuse in its environment, and hence the information available from its emission.

The fluorescence quantum yield is the ratio of the number of photons emitted to the number of photons absorbed. The process governed by the rate constants Γ and k_{nr} both depopulate the excited state. The fraction of fluorophores which decay through emission, and hence the quantum yield, is given by

$$Q = \frac{\Gamma}{\Gamma + k_{nr}} \tag{5.1}$$

The lifetime of the excited state is defined by the average time the molecule spends in the excited state prior to return to the ground state. For the fluorophore, the lifetime is

$$\tau = \frac{1}{\Gamma + k_{nr}} \tag{5.2}$$

Here, it is important to note that the lifetime is an average value of the time spent in the excited state.

Fluorescence measurements can be broadly classified into two types of measurements, steady-state measurement and time-resolved measurements. Steady-state measurements are those performed with constant illumination and observation. This is most common type of measurement. The sample is illuminated with a continuous beam of light, and the intensity or emission spectrum is recorded. Because of nanosecond timescale of fluorescence, most measurements are steady-state measurements. When the sample is first exposed to light, steady-state is reached almost immediately. The second type of measurements, time-resolved measurements, is used for measuring intensity decays or anisotropy decays. For these measurements, the sample is exposed to a pulse of light, where the pulse width is typically shorter than the decay time of the sample. This intensity decay is recorded with a high-speed detection system that permits the intensity or anisotropy to be measured on the nanosecond timescale. It is important to understand that there exists a rather simple relationship between steady-state and time-resolved measurements. The steady-state observation is simply an average of the time-resolved phenomena over the intensity decay of the sample. Considering a fluorophore which displaying a single decay time (τ) and a single rotational correlation time (θ). The intensity and anisotropy decays are given by

$$I(t) = I_0 e^{-\frac{t}{\tau}} \tag{5.3}$$

$$r(t) = r_0 e^{-\frac{t}{\theta}} \tag{5.4}$$

where I_0 and r_0 are, respectively, the intensities and anisotropies at t = 0, immediately following the excitation pulse.

5.3 Determination of Aggregation Number by Fluorescence Spectroscopy of Dodecyl Benzene Sulfonate (DBS) Micelles with Varying Counter Ions

5.3.1. Introduction and review of the previous work

One of the most fundamental and important structural parameters of micellar aggregates is the aggregation number, or the average aggregation number of detergent molecules in micelle unit [1]. Therefore, the measurement and establishment of aggregation number is of great significance in surface science. "**An aggregation number is a description of the number of molecules present in a micelle once the critical micelle concentration (cmc) has been reached**". The fluorescence probe technique is becoming increasingly popular in the study of surfactant micellization/ adsorption [2-6], polymer-surfactant interactions [7-9], microemulsions [10] and determination of aggregation number of the micelle. The value of the aggregation number contains information on the micellar size and shape, which may be important in determining stability and practical applications of the investigated systems [1,11-12]. Methods which permits easy and reliable estimates of micelle aggregation numbers in actual experimental conditions, that is at a given surfactant concentration and in presence of additives such as electrolytes, small organic molecules, polymers or proteins are therefore great interest. Many methods have been used to determine micelle aggregation number [13]. However most of these methods are restricted to small values of the aggregation number (thermodynamic methods, NMR) or suffer from the fact that the measured property depends on the micelle aggregation number and also on the micelle shape and intermolecular interactions (scattering methods). To extract the value of the aggregation number, the result must be extrapolated to low concentration, close to the cmc. In doing so one is likely to modify the micelle size as it is concentration dependent in most surfactant systems. Small angle neutron scattering data at high scattering wave vectors permit in principle the determination of micelle aggregation numbers and also yield information on the micelle shape in the actual experimental conditions [14-15]. However the measurements use experimental setups that are available only in a few facilities in the world, in addition of being very costly. The fluorescent probing method circumvents most of the problems just discussed and permits determinations of micelle aggregation numbers under the actual experimental conditions [16-21]. Indeed, this determination is affected neither by intermicellar

interactions nor by the micellar shape. Besides, the apparatuses required for the measurements are available in most of the university campuses or industrial laboratories. Fluorescence probing methods can also yield information on the micelle polydispersity and micelle dynamics. That is why the luminescent probe technique is becoming increasingly popular in the study of determination of aggregation number of surfactants.

5.3.2. Theory

In the present study, the measurement of aggregation number is done by a simple process based on the quenching of a luminescent probe by a hydrophobic quencher. A typical experiment to determine the mean aggregation number would involve the use of a luminescent probe, quencher and a known concentration of surfactant. If the concentration of the quencher is varied, and the cmc of the surfactant known, the mean aggregation number can be easily determined. Here the word luminescent means the emission of light by a substance not resulting from heat; it is thus from a cold body radiation. The term "luminescence" was introduced in 1888 by Eilhard Wiedemann [22]. Quenching refers to any process which decreases the fluorescence intensity of a given substance. The excited states can be deactivated in several ways - they can emit, giving off light energy, deactivate- resulting in a "vibrationally hot" ground state (i.e., energy loss as heat) or can be quenched by other molecules. A variety of process can result in quenching, such as excited state reactions, energy transfer, complex-formation and collisional quenching. Quenching of the excited state is a significant process because it is usually a very efficient process. Quenching process can occur by two ways – electron transfer or energy transfer. In both the cases, the excited state energy of the luminophore (the luminescent species) is deactivated due to presence of the quencher. Quenching is the basis for fluorescence resonance energy transfer (FRET) assays. There are two types of quenching in fluorescence, viz., "static" and "dynamic" quenching. Static quenching occurs when the donor and acceptor molecules are in the ground state. The donor and acceptor molecules bind together to form a ground state complex, an intramolecular dimer with its unique properties, such as being nonfluorescent and having a unique absorption spectrum. However, if the quencher is somehow associated with the luminophore in solution prior to light absorption, the association may mean that the luminophore will

not emit, due to induced changes in its properties because of presence of quencher. Therefore the reduction in emission intensity will be affected by the extent to which the quencher associates to the luminophore and the number of quenchers present. Whereas, dynamic quenching which occurs by the quencher diffusing through solution and interacting with luminophore, resulting in a deactivation of the excited state. The emission intensity is reduced, because as well as other deactivation pathway in competition with luminescence. This quenching process is controlled by how fast the quencher can diffuse through solution and "collide" with luminophore, and as diffusion is usually a very fast process in solutions, it can be very efficient. The reduction in emission intensity can be quantified as follows. If the luminophore, M, associates with quencher, Q according to an equilibrium constant of association, K_{SV}, then this association constant can be quantified as the ratio of associated luminophore-quenchers moieties ($[M-Q]$) to the product of unassociated luminophore and quencher; $[M][Q]$. Since the total concentration of luminophore, $[M]_0$ is equal to the sum of associated and unassociated luminophore, substitution of this into the equilibrium expression, followed by rearrangement results in another equation of a straight line, very similar in form to the Stern-Volmer equation. However, while plotting $\frac{I_0}{I}$ (as emission intensity can be said to be proportional to concentration) against $[Q]$ will result in a straight line for static quenching, analogous to dynamic quenching, interpretation of the slope is different. In this case, the slope quantifies the association constant between quencher and luminophore - and therefore is useful in providing information on how these two species interact in the ground state. So, the derived equation for static quenching is as follows:

$$\frac{[M]_0}{[M]} = \frac{I_0}{I} = 1 + K_{SV}[Q] \tag{5.5}$$

If we divide the emission quantum yield in the absence of quencher by that in the presence of quencher, we can also generate an expression known as the Stern-Volmer equation for dynamic quenching. The equation is as follows:

$$\frac{\Phi_f^0}{\Phi_f} = \frac{I_f^0}{I_f} = \frac{\tau_0}{\tau} = 1 + K_q\tau_0[Q] \tag{5.6}$$

The derivation of the Stern-Volmer Equation based on considering the rate constants of deactivation in the absence and presence of quencher in this process. So, the Stern-Volmer model is called the dynamic quenching when quenching which occurs by the quencher diffusing through solution and interacting with luminophore, resulting in a deactivation of the excited state. The Stern-Volmer equation is the equation of straight line, and hence it allows for very easy experimental determination of the quenching rate constant, . If the emission intensity (or lifetime) in the absence of quencher and then in the presence of incremental amounts of quencher is measured, and the resulting ratio of emission intensities (/I) is plotted as a function of quencher concentration, the resulting graph (called a Stern-Volmer plot) will have an intercept of 1 and a slope called the Stern-Volmer constant, . is the product of the natural radiative lifetime (the lifetime in the absence of quencher), , and the quenching rate constant, . Knowing the slope and the natural radiative lifetime allows easy calculation of the quenching rate constant. So, dynamic quenching results from collisions between excited state and quencher. In an experiment there is a possibility that the reaction can occur through static quenching or dynamic quenching. The static and dynamic quenching can be represented by a very simple diagram given in figure 5.1.

Figure 5.1: Dynamic and Static Quenching.

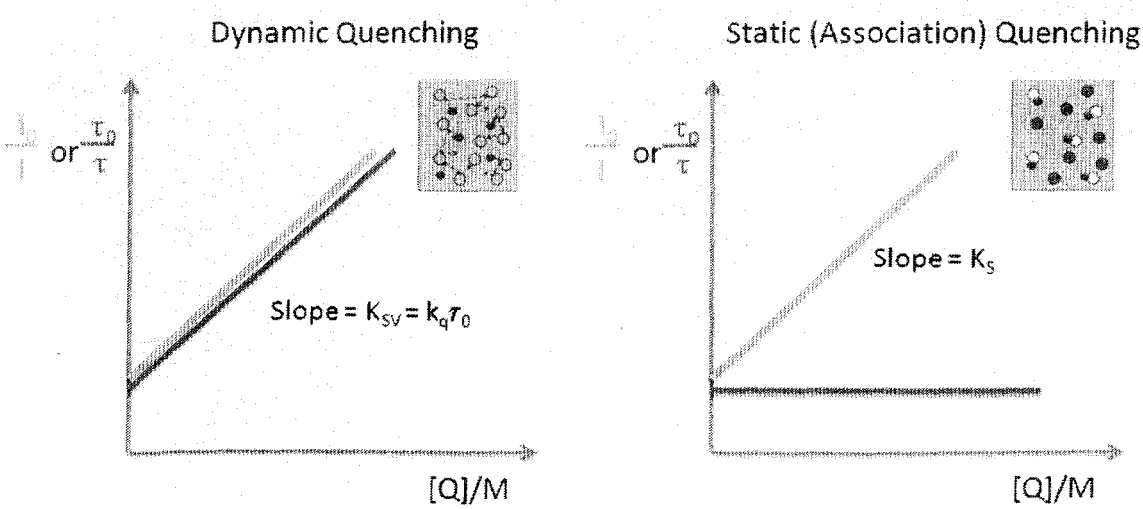

In literature, there are reactions in which both the quenching process, i.e., static and dynamic quenching can occur simultaneously. We can easily understand what type of

quenching process is going on in the reaction. For dynamic quenching, all luminophores are affected by the quenching process as it is probable that they will all collide with a quencher during their excited state lifetime, so both emission intensity and life time reduced on increasing quencher concentration. For static quenching by association, only luminophore-quencher association results in reduction in emission, unassociated luminophores are free to luminescence as if there was no quencher present. Increasing quencher concentration affects emission intensity, because there are more associations, but not emission lifetime, as the unassociated luminophores can emit in the absence of quencher.

In the present experiment, the static quenching is done to measure the aggregation number of the surfactant with different counterions by steady state fluorescence quenching (SSFQ) process. This work is a part of program in our laboratory to study the dodecyl benzene sulfonate micelle as the counterion is symmetrically made more bulky and hydrophobic. It is also known that the hydration layer, so-called the Stern layer, exists in the interface between the hydrophobic micelle core and bulk water. This layer consists of the ionic head groups, counterions and hydrated water molecules. The layer should play an important role for the structural stability and dynamical property of micelle in water. Here we study sodium-, Lithium, Potassium-, Ammonium-, Tetramethyl ammonium-, Tetraethyl ammonium-, Tetrapropyl ammonium- and Tetrabutylammoniumdodecylbenzene sulfonate micelle aggregation number.

The probe was dissolved in trace amount ($< 10^{-6}$ μM) in aqueous solution in a series of surfactant having different counterions. The method involves the use of a hydrophobic substance which exhibits different fluorescence characteristics depending upon the properties of the solubilising medium. For example, fluorescence probe, in our case pyrene, are sensitive to the polarity of the solubilising medium will exhibit different fluorescence behaviour in micellar and nonmicellar solutions. Such changes of behaviour as a function of surfactant concentration have been used to determine the micelle characteristics of certain surfactants. The schematic representations of pyrene and cetyl pridinium chloride are given in the figure 5.2 and figure 5.3 below:

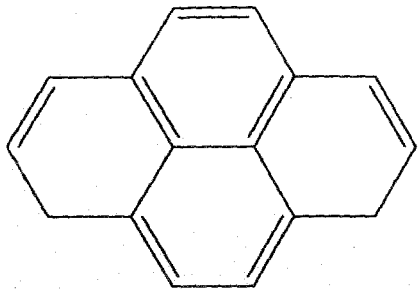

Figure 5. 2. Structure of Pyrene

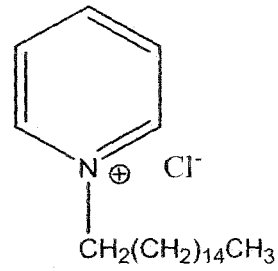

Figure 5.3 -Hexadecylpyridinium chloride (CPC)

5. 3.3. Materials and method

LDBS, PDBS, ADBS, TMADBS, TEADBS, TPADBS and TBADBS were prepared from a sample of purified SDBS by ion exchange as described in the Chapter III. Pyrene and CPC were of puriss grade (Fluka, Switzerland) used as received.

Method

Preparation of Pyrene solution

A pyrene stock solution (5 μM) is prepared as follows: About 2.02 mg of pyrene is dissolved in 10 ml absolute alcohol. 8.81 ml of this solution is added to a volumetric flask already containing 75 ml pure distilled water and the volume is made upto 100 ml with pure distilled water. Then the solution which is white in colour and turbid in nature was sonicated for 50 minutes. 0.5 ml of this turbid, white solution was then poured into another 100 ml volumetric flask containing about 50 ml pure distilled water and the volume made upto 100 ml by diluting with pure distilled water. The solution further sonicated upto 10 minutes.

The aggregation number of micelle was determined by the steady-state fluorescence quenching method using a Fluorescence Spectrophotometer, viz., Photon Technology International Co., USA (Model Q 40). Pyrene (5×10^{-6} μM) was used as a probe and CPC as a quencher. Emission spectra of Pyrene were obtained by exciting the samples at 332 nm and emission was measured in the range of 350-520 nm. The emission peak at 393 nm is considered for our calculation of the ratio of intensity.

5.3.4. Results and Discussion

The fluorescence spectrum of pyrene in water exhibits five predominant peaks. It has been shown in the case of pyrene, a quencher used to measure the aggregation number, that the ratio of intensity of the first (I_1 at 373nm) and third peaks (I_3 at 384 nm) is a sensitive parameter characterizing the polarity of the probe environment. For example, I_1/I_3 in hydrocarbon solvents has a value of about 0.6, in ethanol about 1.1, and in water about 1.8. The value of I_1/I_3 remains constant upto a certain surfactant concentration and decrease sharply above it. A lowering of the value of I_1/I_3 is an indication of the solubilization of the probes in a more hydrophobic environment than water and in this case it is surfactant micelle and also with the quencher [23]. The aggregation number of the surfactant was determined by the static fluorescence quenching method using the following equation and also considering the usual following assumptions:

(I) Static quenching occurs between the fluorescence probe and the quencher molecules so the quenching process does not affect the fluorescence lifetime of the probe.

(II) Fluorescence lifetime of the probe is much less than the residence times of the quencher and probe inside the micelle.

(III) The probability of finding a micelle with more than one probe molecule is negligible as because the quencher concentration is very low.

Following Poisson statistics [24] for the description of probe and the quencher among the micelles, the logarithm of I_0/I takes the form

$$\ln \frac{I_0}{I} = \frac{[Q]N}{([S]_0 - cmc)} \qquad (5.7)$$

where, I_0 and I are the intensities of fluorescence without and with quencher. $[Q]$ is the bulk quencher concentration, N is the mean aggregation number and $[S]_0$ is the total surfactant concentration. The aggregation number has been obtained by plotting $\ln \frac{I_0}{I}$ as a function of quencher concentration.

In the present study, good linear plots for all the surfactants have been obtained satisfying the above equation suggesting constancy of both N and K_{SV}. The

plots of fluorescence measurement for surfactant with different counter ions are shown from figure 5.4 to figure 5.11.

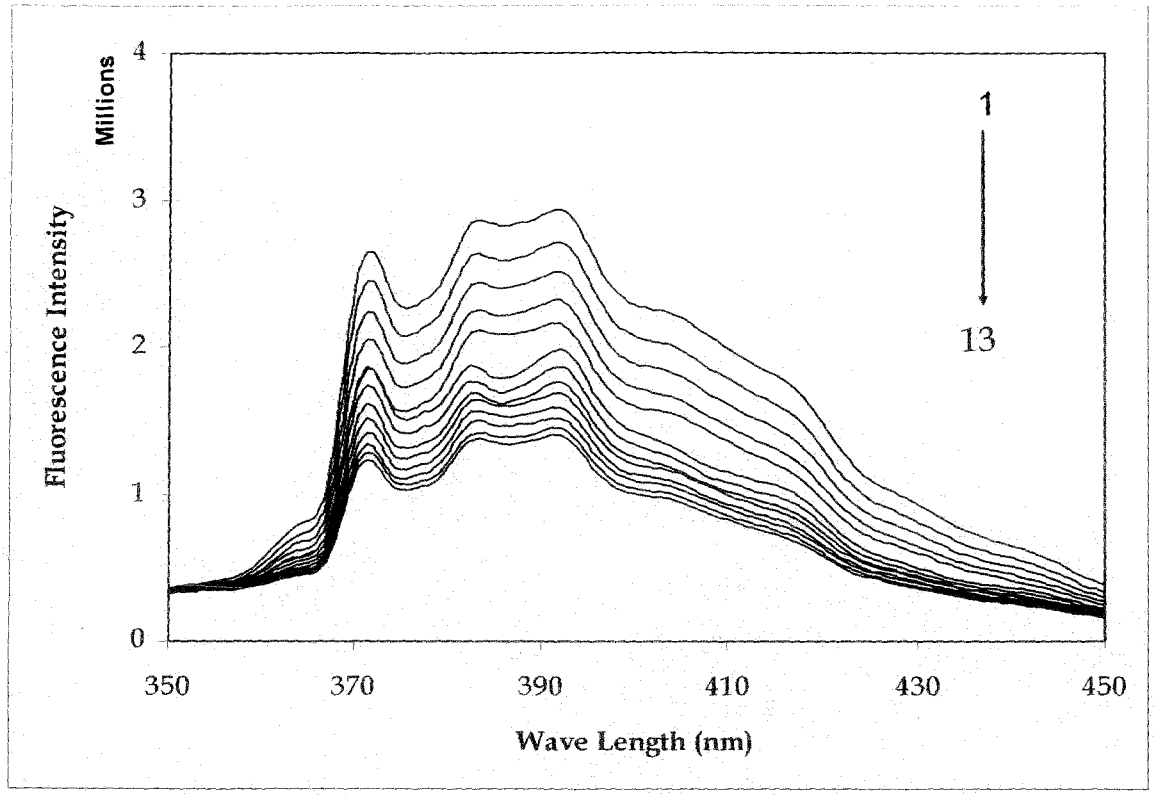

Figure 5.4(a): Fluorescence Spectra of pyrene in sodium dodecyl benzene sulfonate with different concentration of CPC in mM (1) 0.0 mM (2) 0.0054 mM (3) 0.105 mM (4) 0.152 mM (5) 0.196 mM (6) 0.237 mM (7) 0.276 mM (8) 0.312 mM (9) 0.346 mM (10) 0.379 mM (11) 0.409 (12) 0.438 mM (13) 0.466 mM

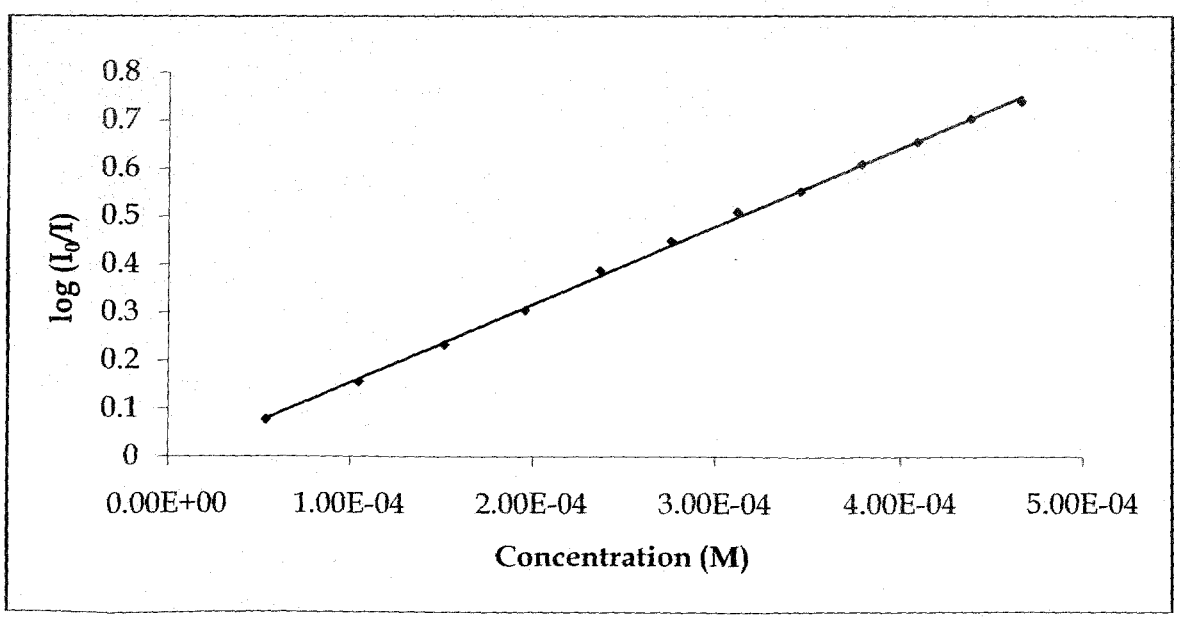

Figure5.4(b): Log (I_0/I) Vs Concentration (M) plot of Sodium dodecyl benzene sulfonate.

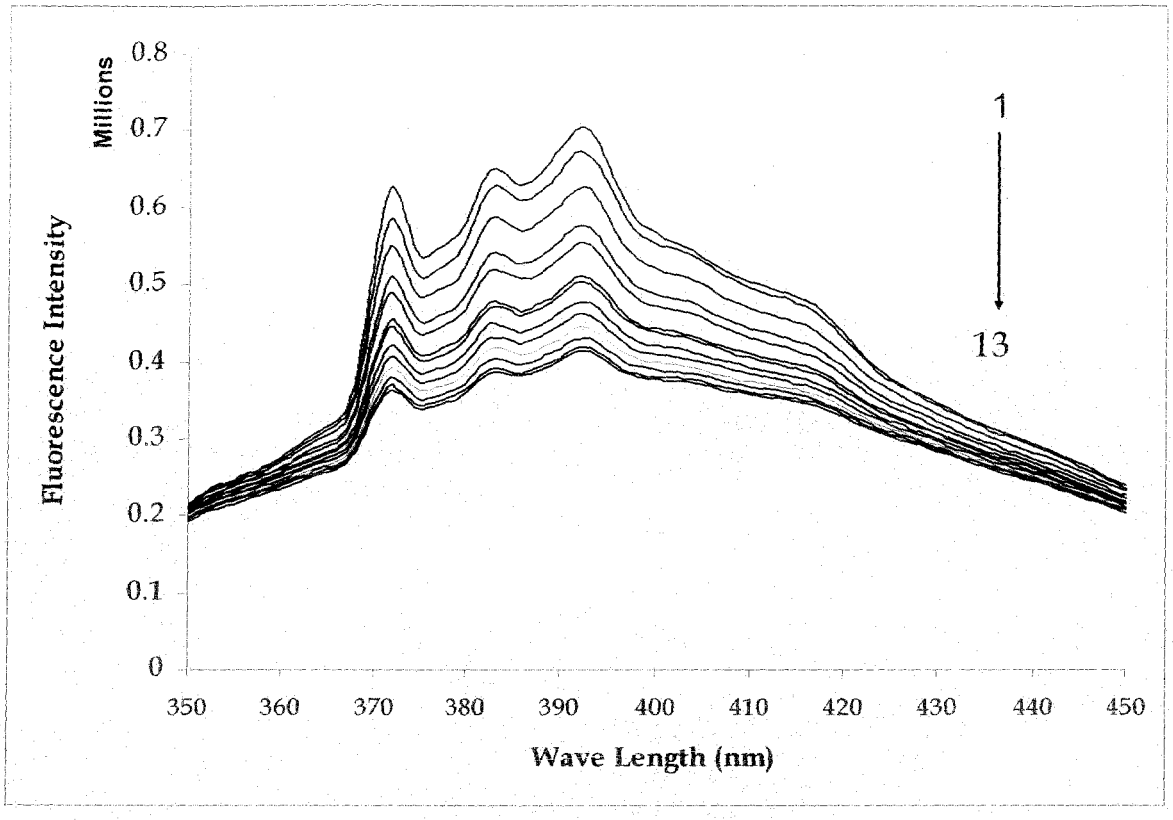

Figure 5.5(a): Fluorescence Spectra of pyrene in lithium dodecyl benzene sulfonate with different concentration of CPC in mM (1) 0.0 mM (2) 0.0054 mM (3) 0.105 mM (4) 0.152 mM (5) 0.196 mM (6) 0.237 mM (7) 0.276 mM (8) 0.312 mM (9) 0.346 mM (10) 0.379 mM (11) 0.409 (12) 0.438 mM (13) 0.466 mM

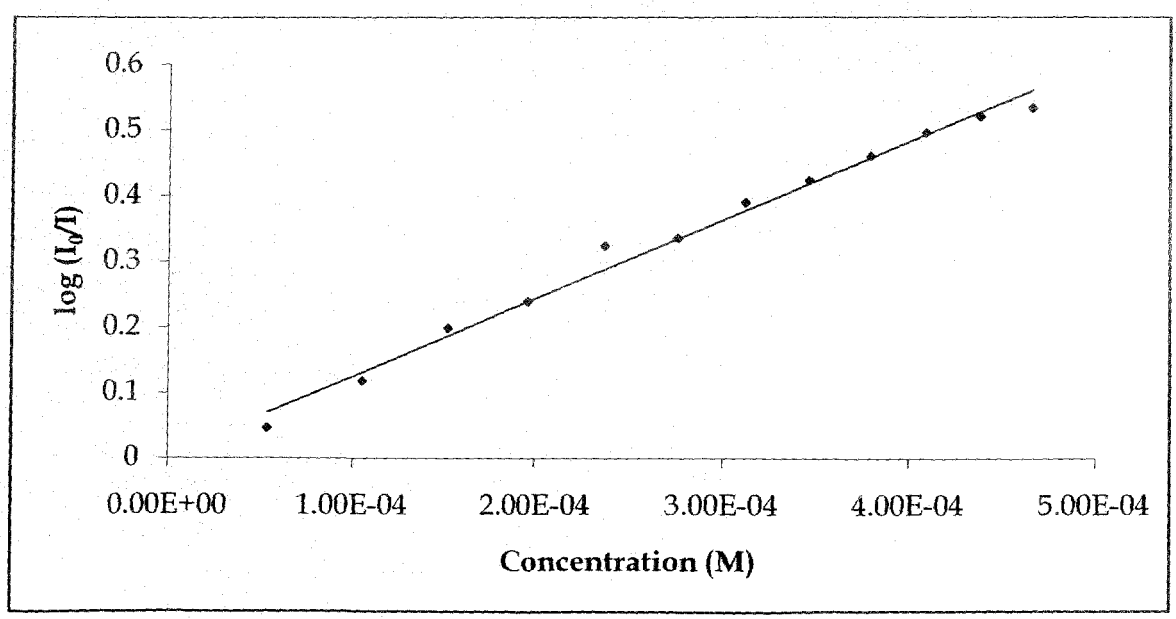

Figure 5.5(b):: Log (I_0/I) Vs Concentration (M) plot of Lithium dodecyl benzene sulfonate.

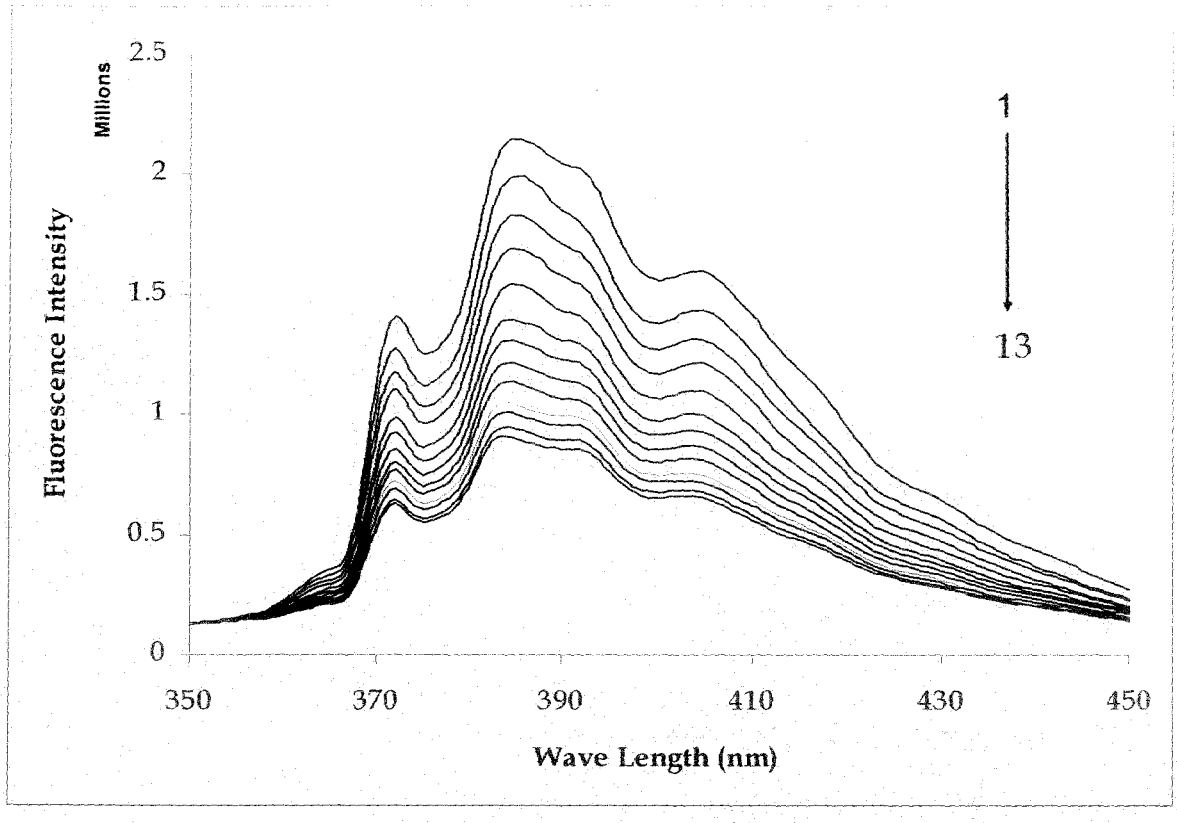

Figure 5.6(a): Fluorescence Spectra of pyrene in potassium dodecyl benzene sulfonate with different concentration of CPC in mM (1) 0.0 mM (2) 0.0054 mM (3) 0.105 mM (4) 0.152 mM (5) 0.196 mM (6) 0.237 mM (7) 0.276 mM (8) 0.312 mM (9) 0.346 mM (10) 0.379 mM (11) 0.409 (12) 0.438 mM (13) 0.466 mM

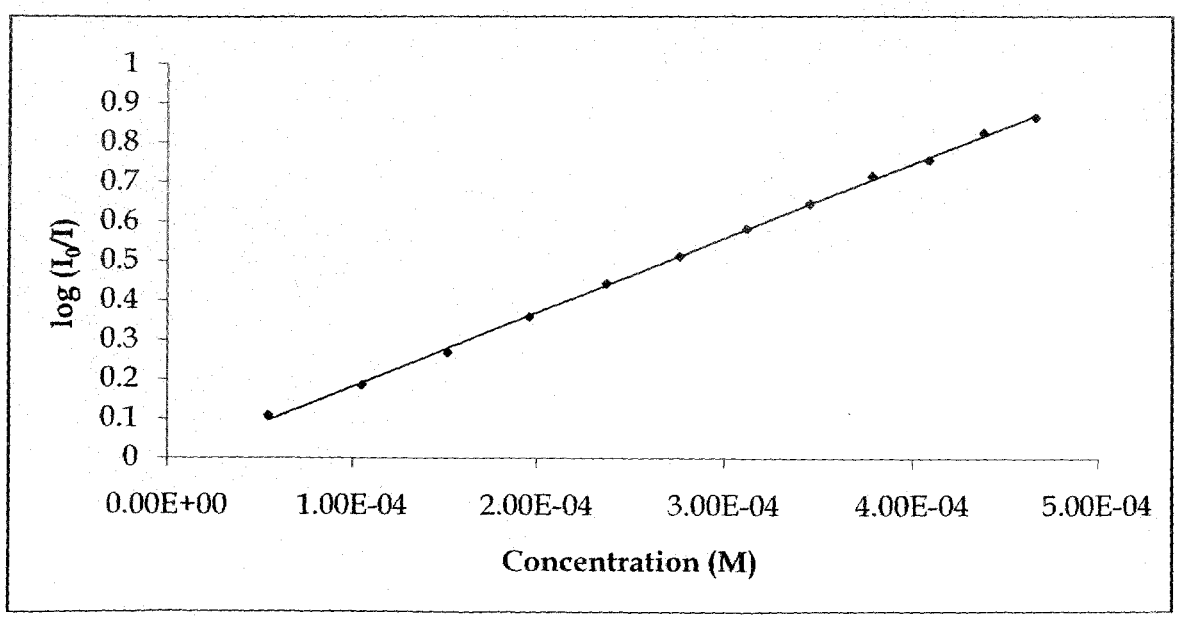

Figure 5.6(b): Log (I_0/I) Vs Concentration (M) plot of Potassium dodecyl benzene sulfonate.

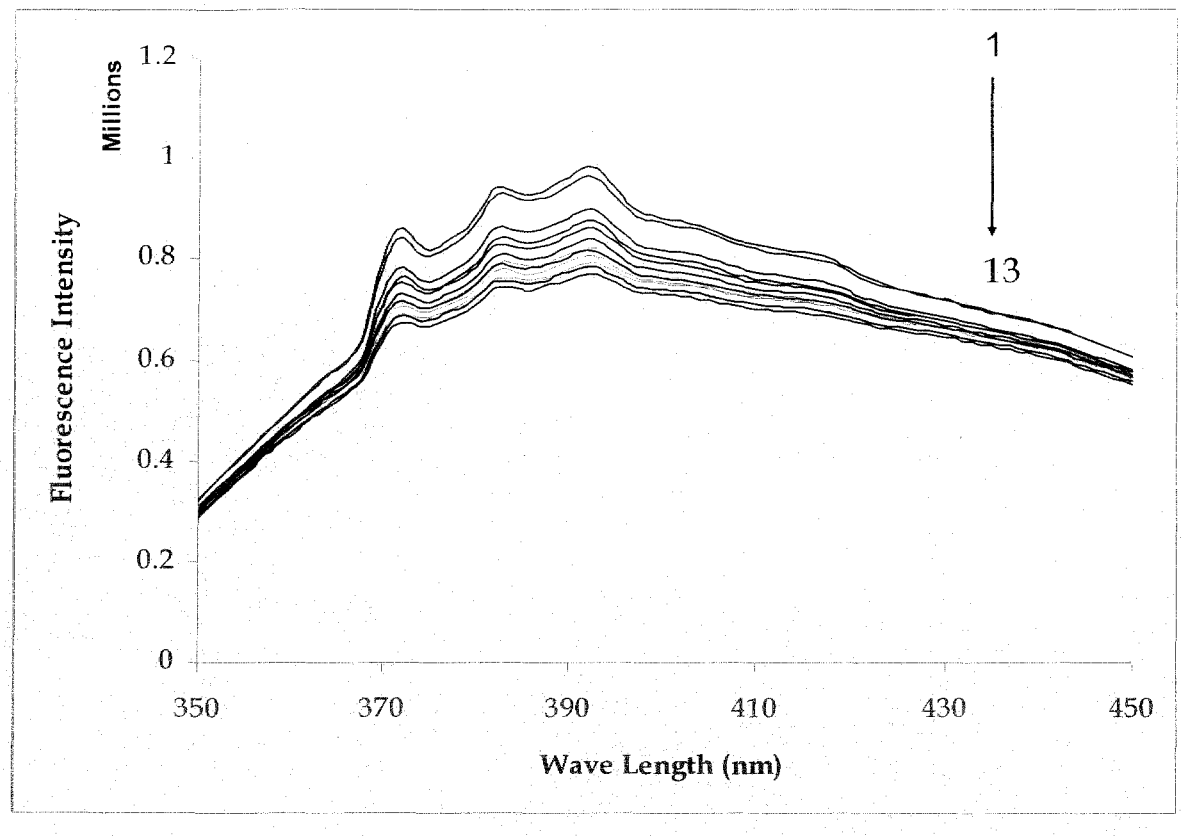

Figure 5.7(a): Fluorescence Spectra of pyrene in ammonium dodecyl benzene sulfonate with different concentration of CPC in mM (1) 0.0 mM (2) 0.0054 mM (3) 0.105 mM (4) 0.152 mM (5) 0.196 mM (6) 0.237 mM (7) 0.276 mM (8) 0.312 mM (9) 0.346 mM (10) 0.379 mM (11) 0.409 (12) 0.438 mM (13) 0.466 mM

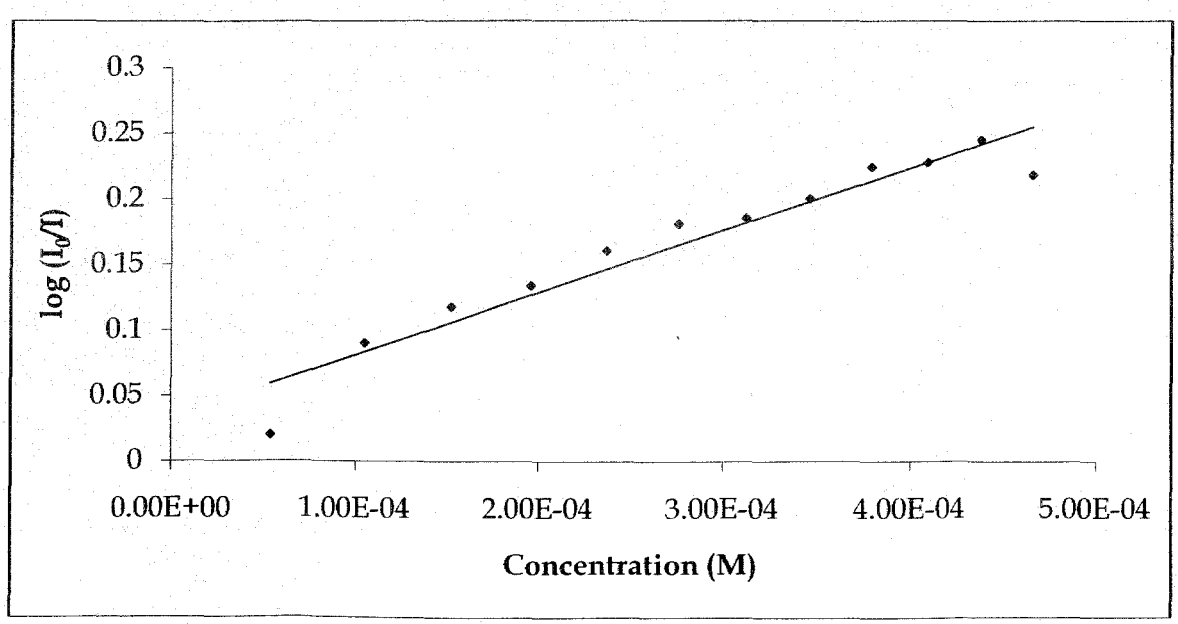

Figure 5.7(b): Log (I_0/I) Vs Concentration (M) plot of Ammonium dodecyl benzene sulfonate.

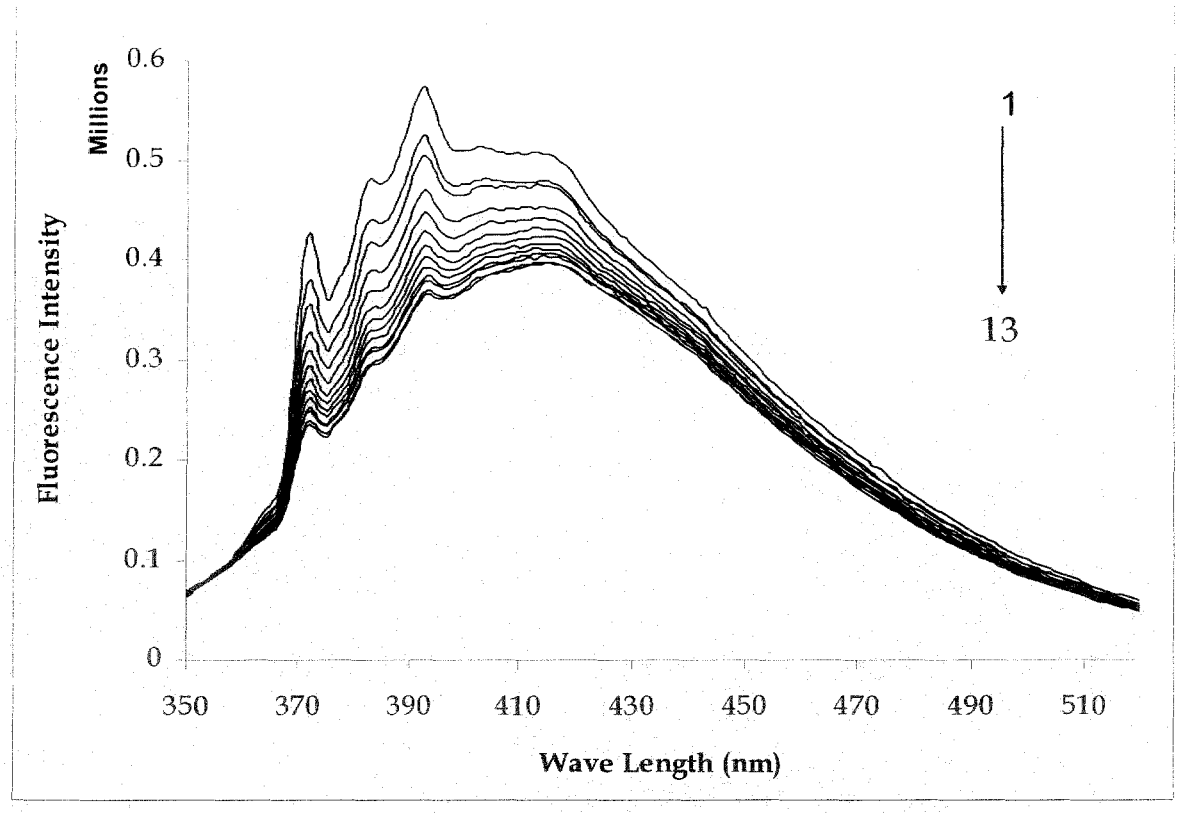

Figure 5.8(a): Fluorescence Spectra of pyrene in tetramethyl ammonium dodecyl benzene sulfonate with different concentration of CPC in mM (1) 0.0 mM (2) 0.0054 mM (3) 0.105 mM (4) 0.152 mM (5) 0.196 mM (6) 0.237 mM (7) 0.276 mM (8) 0.312 mM (9) 0.346 mM (10) 0.379 mM (11) 0.409 (12) 0.438 mM (13) 0.466 mM

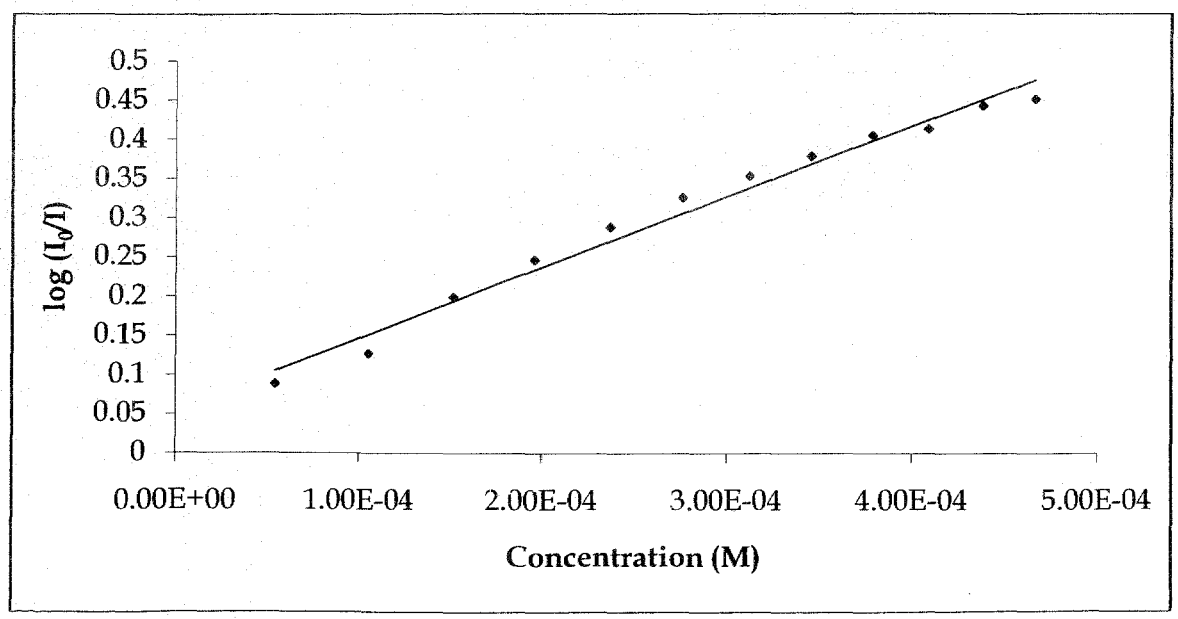

Figure 5.8(b): Log (I_0/I) Vs Concentration (M) plot of Tetramethyl ammonium dodecyl benzene sulfonate.

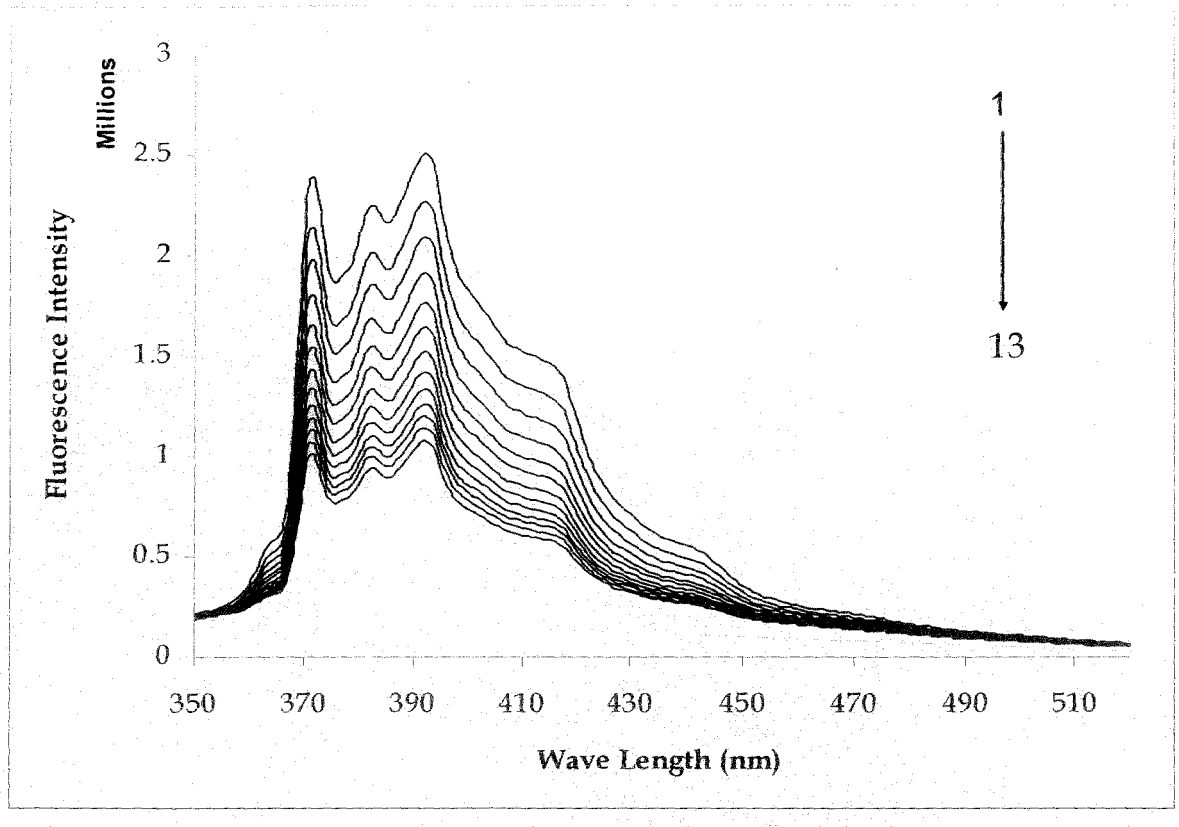

Figure 5.9(a): Fluorescence Spectra of pyrene in tetraethyl ammonium dodecyl benzene sulfonate with different concentration of CPC in mM (1) 0.0 mM (2) 0.0054 mM (3) 0.105 mM (4) 0.152 mM (5) 0.196 mM (6) 0.237 mM (7) 0.276 mM (8) 0.312 mM (9) 0.346 mM (10) 0.379 mM (11) 0.409 (12) 0.438 mM (13) 0.466 mM

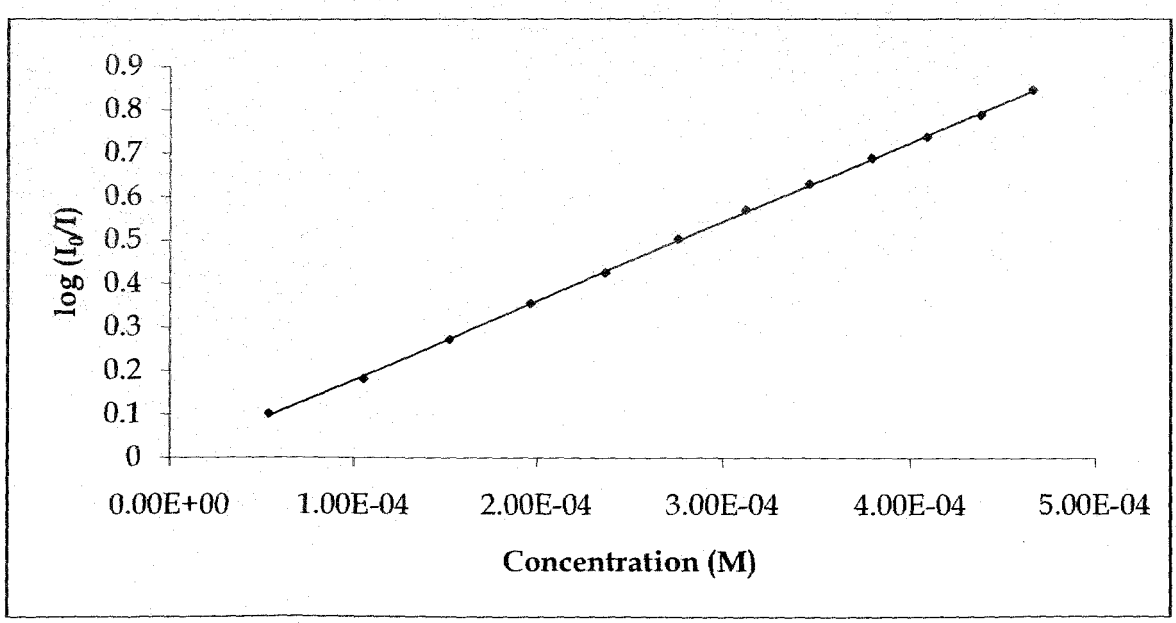

Figure 5.9(b): Log (I_0/I) Vs Concentration (M) plot of Tetraethyl ammonium dodecyl benzene sulfonate.

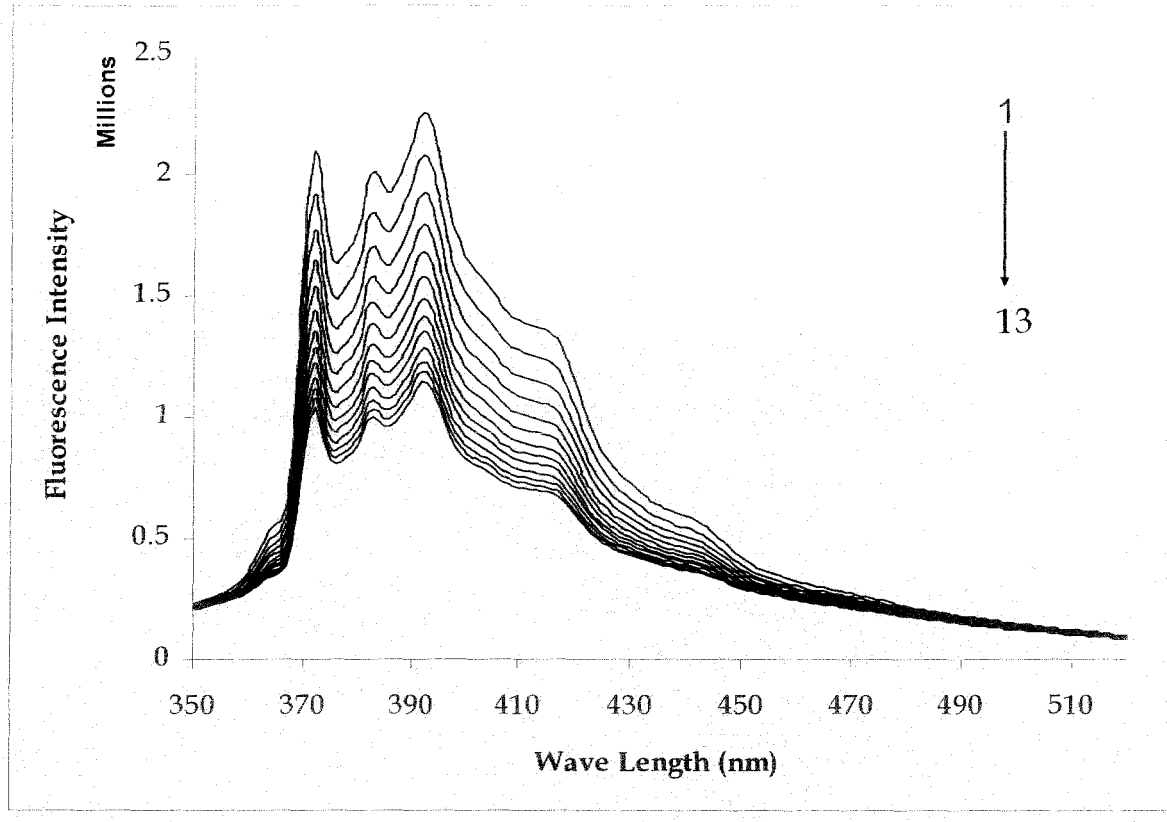

Figure 5.10(a): Fluorescence Spectra of pyrene in tetrapropyl ammonium dodecyl benzene sulfonate with different concentration of CPC in mM (1) 0.0 mM (2) 0.0054 mM (3) 0.105 mM (4) 0.152 mM (5) 0.196 mM (6) 0.237 mM (7) 0.276 mM (8) 0.312 mM (9) 0.346 mM (10) 0.379 mM (11) 0.409 (12) 0.438 mM (13) 0.466 mM

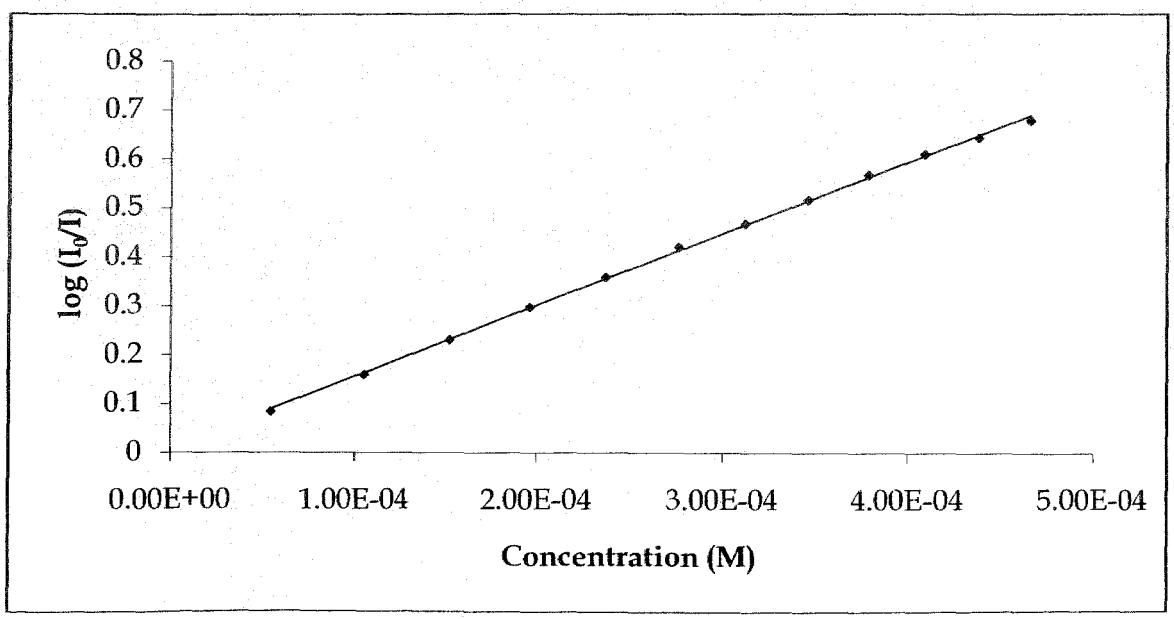

Figure 5.10(b): Log (I_0/I) Vs Concentration (M) plot of Tetrapropyl ammonium dodecyl benzene sulfonate.

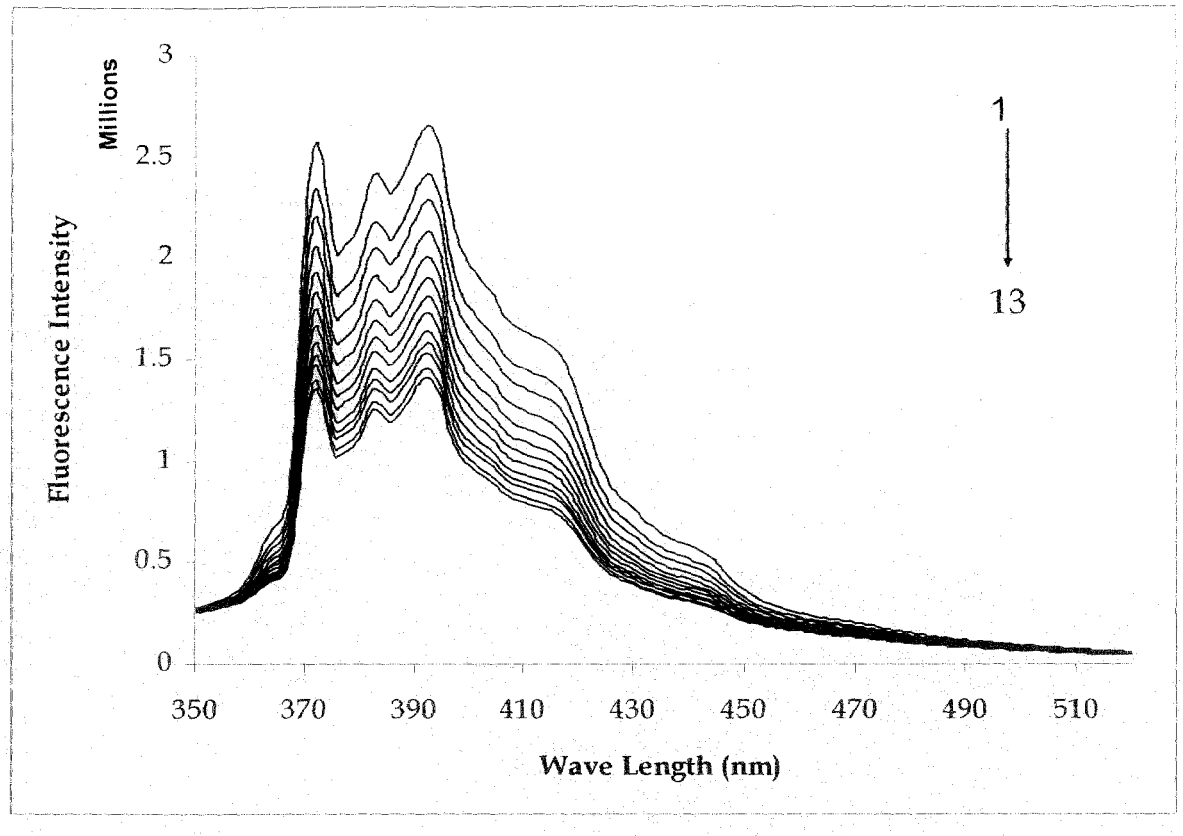

Figure 5.11(a): Fluorescence Spectra of pyrene in tetrabutyl ammonium dodecyl benzene sulfonate with different concentration of CPC in mM (1) 0.0 mM (2) 0.0054 mM (3) 0.105 mM (4) 0.152 mM (5) 0.196 mM (6) 0.237 mM (7) 0.276 mM (8) 0.312 mM (9) 0.346 mM (10) 0.379 mM (11) 0.409 (12) 0.438 mM (13) 0.466 mM

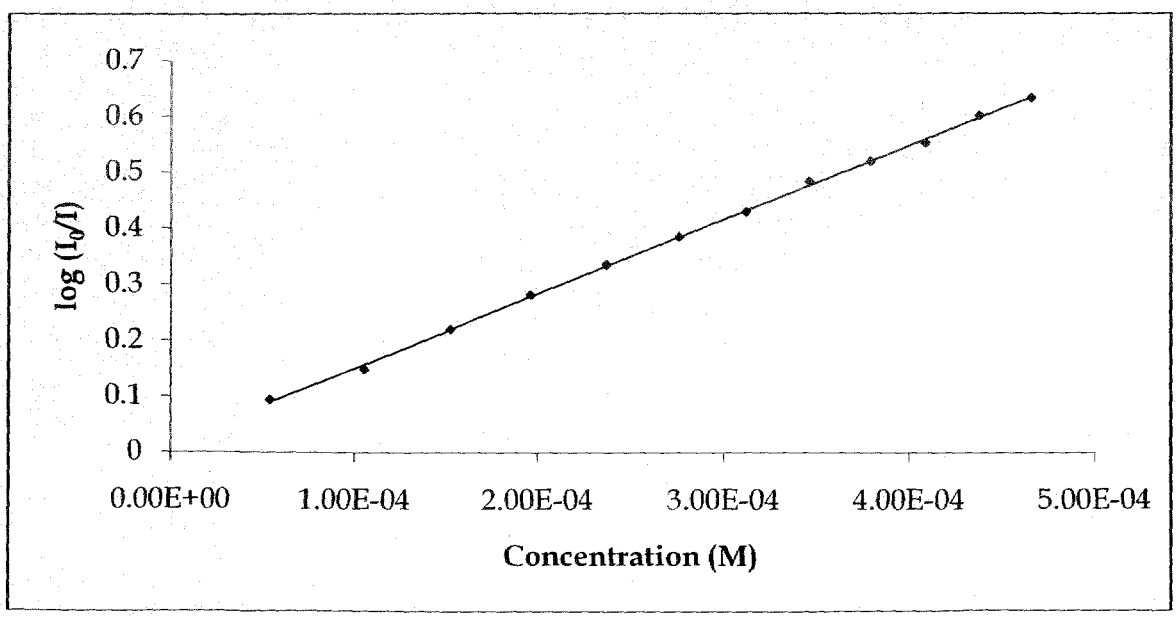

Figure 5.11(b): Log (I_0/I) Vs Concentration (M) plot of Tetrabutyl ammonium dodecyl benzene sulfonate.

The ratio of the intensities (I_0/I_Q) of fluorescence emission of pyrene in absence (I_0) and presence (I_Q) of the quencher of surfactant with different counter ions and aggregation number measured at 298 K for all the surfactants in aqueous solutions are given in table 5.1 and table 5.2.

Table 5.1

Ratio of the intensities (I_0/I_Q) of fluorescence emission of pyrene in the absence (I_0) and presence (I_Q) of the quencher (CPC) at 373 nm in aqueous solution of dodecyl benzene sulfonate with different counterions at 298 K

[CPC]	Ratio of the intensities of surfactant with different counterions (I_0/I_Q)							
mM	Na^+	Li^+	K^+	NH_4^+	TMA^+	TEA^+	TPA^+	TBA^+
0.0000	1.0000	1.0000	1.0000	1.0000	1.0000	1.0000	1.0000	1.0000
0.0540	1.0812	1.0469	1.1144	1.0204	1.0921	1.1064	1.0882	1.0882
0.1050	1.1695	1.1251	1.2034	1.0945	1.1354	1.1993	1.1739	1.1739
0.1520	1.2630	1.2194	1.3057	1.1250	1.2198	1.3125	1.2599	1.2599
0.1960	1.3570	1.2700	1.4305	1.1429	1.2784	1.4249	1.3465	1.3465
0.2370	1.4747	1.3812	1.5572	1.1739	1.3333	1.5280	1.4314	1.4314
0.2760	1.5669	1.3984	1.6663	1.1982	1.3837	1.6505	1.5209	1.5209
0.3120	1.6648	1.4765	1.7866	1.2035	1.4225	1.7655	1.5958	1.5958
0.3460	1.7383	1.5264	1.9034	1.2216	1.4593	1.8756	1.6749	1.6749
0.3790	1.8388	1.5831	2.0410	1.2515	1.4983	1.9900	1.7624	1.7624
0.4090	1.9259	1.6406	2.1240	1.2560	1.5110	2.0889	1.8390	1.8390
0.4380	2.0207	1.6814	2.2767	1.2780	1.5568	2.1966	1.9018	1.9018
0.4660	2.0936	1.7038	2.3688	1.2440	1.5703	2.3287	1.9698	1.9698

From the table, it is very clear that the ratio of emission intensity of pyrene changes with the counterions present with the dodecyl benzene sulfonate group of the surfactant.

Table 5.2.
Aggregation number of the dodecyl benzene sulfonate with different counterions at temperature 298 K.

Surfactant	Temp./K	Agg. No. (N_0)
Sodium Dodecyl Benzene Sulfonate (SDBS)	298	27
Lithium Dodecyl Benzene Sulfonate (LDBS)	298	20
Potassium Dodecyl Benzene Sulfonate (PDBS)	298	33
Ammonium Dodecyl Benzene Sulfonate (ADBS)	298	08
Tetramethyl Ammonium Dodecyl Benzene Sulfonate (TMADBS)	298	17
Tetraethyl Ammonium Dodecyl Benzene Sulfonate (TEADBS)	298	34
Tetrapropyl Ammonium Dodecyl Benzene Sulfonate (TPADBS)	298	27
Tetrabutyl Ammonium Dodecyl Benzene Sulfonate (TBADBS)	298	25

Aggregation number increases with alkyl chain length of organic counterions and gives maximum value for tetraethylammonium ion due to hydrophobic interactions of hydrocarbon exterior of the ions with exposed hydrocarbon to the micelle surface. However, for tetrapropyl and tetrabutyl ammonium ions aggregation become increasingly unfavorable due to steric hindrance for increasing counterion size. Here, comparison of aggregation number with ionization degree might be interesting. The ionization degrees of all the surfactants are shown in table 3.2 and table 3.3. The result shows that the values are quite high which indicate that the tetraalkylammonium counter ions are strongly bound to the micelle surface. It is also observed that the counter ion ionization degree increases in the series $NH_4^+ \leq N^+(CH_3)_4 < N^+(C_2H_5)_4 < N^+(C_3H_7)_4 < N^+(C_4H_9)_4$. This means that, as expected, the binding increases as the counter ion becomes more and more hydrophobic in nature. The values of cmc also follow the opposite trend, i.e., as the fraction of counter ion binding increases, the micelles are formed at lower concentrations. However, the aggregation number does not follow the expected trend. At 298 K, the aggregation number become minimum in the case of NH_4^+ counter ion. But as the alkyl groups are substituted for hydrogens, the aggregation number increases because of the formation of larger aggregates which is the consequences of the increased charged screening at higher counter ion binding

capacity via stronger hydrophobic interactions with the micelles. This increasing trend of aggregation number continues up to the tetraethylammonium ions. But for tetrapropyl and tetrabutyl ammonium ions, aggregation number progressively decreases as shown in the table 5.2. This is indeed interesting. Such a complex behaviour of micelle pertaining to the aggregation number with respect to the expected trend on the basis of cmc values is, however, available in the literature [25]. It has been shown that the effect of head group size of tetradecyltrialkylammonium bromide surfactant is very important pertaining to the observed reverse trend of the aggregation number with respect to its cmc. For these surfactants the values of both the cmc and aggregation number, N, decrease as the size of the tetraalkylammonium head group increases. This effect has been explained in terms of the geometric steric hindrance (overlap) between large trialkylammonium head groups at the micellar surface [26-27]. It seems apparent that in the present systems, as the hydrophobicity of the counter ions increases, the counter ion binding/condensation increases due to increased hydrophobic interactions and eventually the cmc decreases. However, enhanced electrostatic charge screening of the head groups is incapable of increasing the aggregation number of the micelles for tetrapropyl and tetrabutylammonium counter ions. On the other hand, micellar surface probably does not offer sufficient surface area to accommodate all the N^+R_4 counter ions that must bind to the micelle to ensure their stability. Therefore, the micelles become smaller in size and more in number to provide larger surface area in order to pack a large number of counter ions. For alkali metal counter ions, hydration plays an important role along with ionization degree. The table 5.2 shows that among the three alkali metal counter ions, lithium yields minimum aggregation number where as potassium ion yields the maximum. However, among all the counter ions, inorganic and organic, ammonium ions display the lowest value of aggregation number of DBS micelles in aqueous medium.

5.4. Studies of Interactions with oxazine dye in aqueous media

5.4.1. Introduction and review of the previous work

Study of the spectroscopic property of organic dyes in a micellar medium is important for understanding the thermal and light induced reactions in biomembranes (28-40). Such reactions proceed through the involvement of excited and free radical species whose behaviour in a micellar medium can be significantly different from that in a homogeneous medium. Cresyl Fast violet, an oxazine dye, has been used as a sensitizer in photo-galvanic devices [41-42]. Dye sensitization of wide band gap semiconductor particles is of current interest particularly for harnessing solar energy and for various other applications [43-47]. The dye surfactant interactions have also been the subject of many studies in view of the fact that they mimic many biological processes taking place between the large organic molecules and biomembrane and can act as a model redox system [48-51]. Further, such interaction between ionic dye and charged surfaces is of interest in numerous applications ranging from the design of electronic devices to the characterization of drug-delivery systems [52]. In view of the above, we have under taken a detailed study to understand the effects of surfactants on the spectroscopic properties of cresyl violet with anionic surfactants because only anionic surfactants have pronounced effect.

In the present experiment, we use an oxazine dye with dodecyl benzene sulfonate with varying counterions. The oxazine dyes display surprising long-wavelength absorption and emission maxima in fluorescence which makes these groups of dye an important fluorescent probe. Extended conjugated systems result in long absorption and emission wavelengths for these types of dye due to their comparatively small size [53-54]. Dyes of this class have been extensively characterized for use as long-wavelength probes and in DNA sequencing [55]. Dyes of this type are also used for staining DNA restriction fragments during capillary electrophoresis. We have studied the stedy-state spectra of surfactants by a typical oxazine dye, Cresyl fast violet. This may be of interest for a number of reasons: it could give a better insight of the nature of interaction in the surfactant aggregate system; it may explain the previously observed temperature dependence of monomer spectra of some dyes [56-57] and none the less, it can test the applicability of the

exciton theory in molecular aggregate systems in further detail. Schematic representation of the dye is given in Figure 5.12.

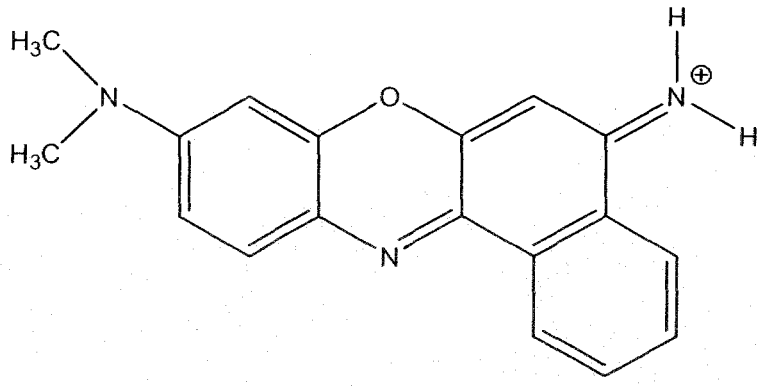

Figure 5.12: Schematic representation of Cresyl Fast Violet (CFV)

5.4.2. Materials and methods

Materials

Cresyl fast Violet (CFV) was supplied by Aldrich Chemical Co., USA and was used after recrystallization from water-ethanol mixture. SDBS was purchased from Acros Organics, USA. (Product code 325912500). Surfactants, viz., LDBS, KDBS, ADBS, TMADBS, TEADBS, TPADBS and TBADBS were prepared in our laboratory by ion-exchange method as discussed in the previous chapter.

Methods

Steady-state emission spectra were done in a Fluorosence Spectrophotometer, Photon Technology Inc. Co., USA. In all the experiment, the concentration of the dye is very low, 1×10^{-6} (M). Quartz cuvettes and double distilled water were employed throughout the experiments. Excitation and emission slit widths were set at 0.20 nm, 0.60 nm, 0.50 nm and 1.50 nm for all the four slits respectively. The excitation wavelength was set at 584 nm for cresyl fast violet solutions. The emission spectra were recorded from 500 nm to 750 nm for all the dye & surfactant mixtures. The emission wave length for the dye is found to be 620 nm.

5.4.3. Results and discussions

The surfactant dodecylbenzene sulfonate consists of hydrophilic ends attached to long nonpolar organic chains. The presence of surfactants increases the free energy of a system by distorting the structure of the water molecules in aqueous solution. In aqueous solutions, micelles are usually spherical with the polar ends on their surfaces and the nonpolar organic chains on the inside. The organic micelle interiors will essentially become pockets of another solvent within the aqueous solution. Nonpolar molecules will tend to migrate into this region and will experience a much different environment there than they would in the bulk aqueous solution.

The spectral characteristics of dyes are known to change when dissolved in surfactant micelles [58-59]. Based on their structures, it is not surprising that DBS moiety and the cresyl fast violet readily interact. All the species have both organic and polar parts, so they can interact with each other through non-polar interactions, polar/ionic interactions or both. Due to these dye-surfactant interactions, the changes in spectral characteristics are observed qualitatively. In this experiment, a very low concentration of dye (~5×10^{-6} M) is used to overcome the effects of dye-dye interactions via possible dimer formation by the dye molecules. In addition to dye-solvent interactions, dye-surfactant and dye-micelle interactions are possible in solutions containing both dye and surfactants [59]. At concentration below the normal cmc, surfactants and dyes can interact to form a mixed micelle of the two species, lowering the resultant cmc. Above the cmc, a change in the molecular environment of the dye due to incorporation into the micelle interior is observed [52].

The fluorescence spectra of the cresyl fast violet vary with surfactant concentration. The spectra of cresyl fast violet without surfactants showed a single peak at 624 nm as shown in the Figure 5.13.

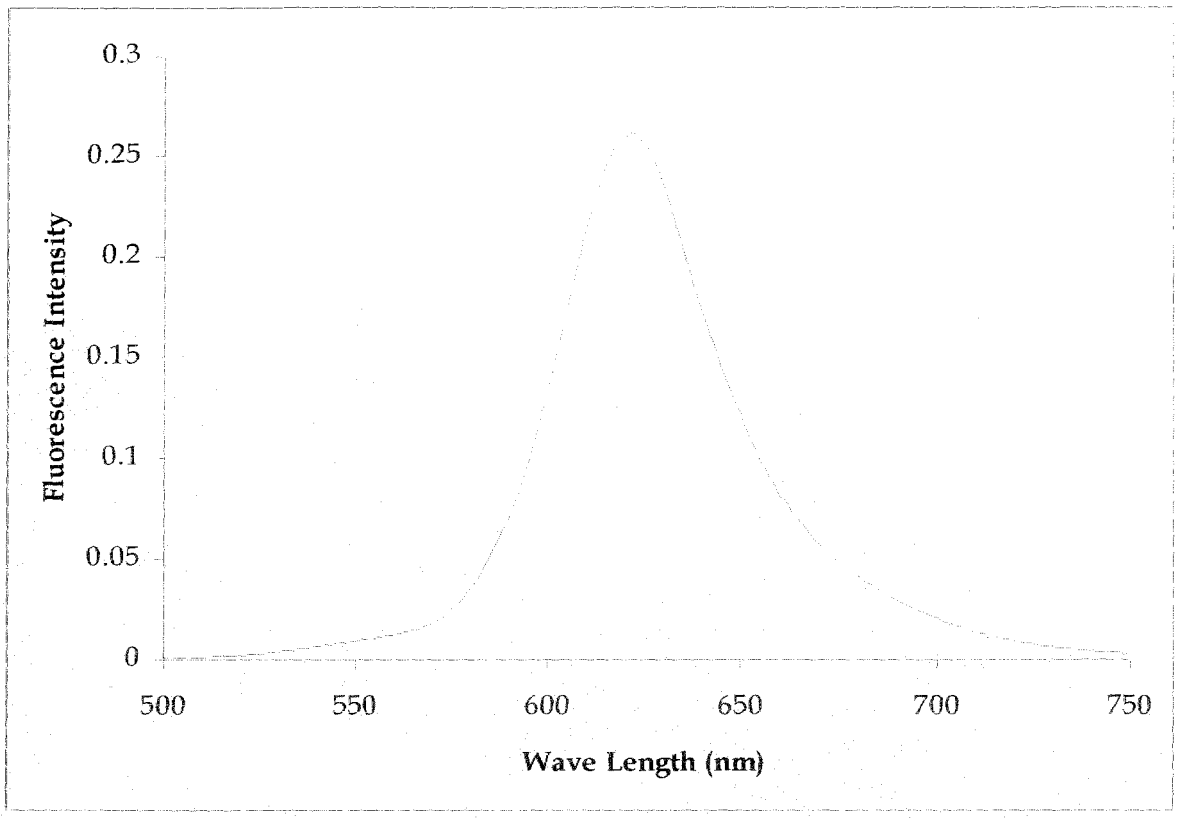

Figure 5.13. Fluorescence emission spectrum of cresyl fast violet (CSV), excitation wave length at 584 nm.

At concentrations of surfactants below the cmc, the fluorescence intensity decreases continuously with increase in surfactant concentration. When the surfactant concentration reaches cmc, the intensity starts increasing continuously with increase in surfactant concentration. The fluorescence spectra of dye in all the surfactant show similar behaviour with the change of surfactant concentrations. However, above cmc, the fluorescence intensities increase. The result suggests that the free monomer is tied up in ion pair or clusters. Above the cmc the fluorescence intensity increases to almost same or very close to that of the cresyl fast violet solution without the surfactant. This shows that above the cmc the dye is freed from the interaction just discussed. Since the emission intensity is same or to some extent lower as compared to the free dye, it may be argued that there was no other interaction between dye and surfactant present. Change in the absorption spectrum and decrease in fluorescence intensities below the cmc's of anionic surfactants could be attributed to the formation of ion-pair complexes of the dye with oppositely charged surfactants. At surfactant concentrations above the cmc the dye band intensity is restored with red shift. Similar result of dye surfactant interaction was also observed by other researchers [52, 58-59].

The steady-state plot of florescence emission intensity vs. wave length for all the surfactants are as follows (figure 5.14 to figure 5.21):

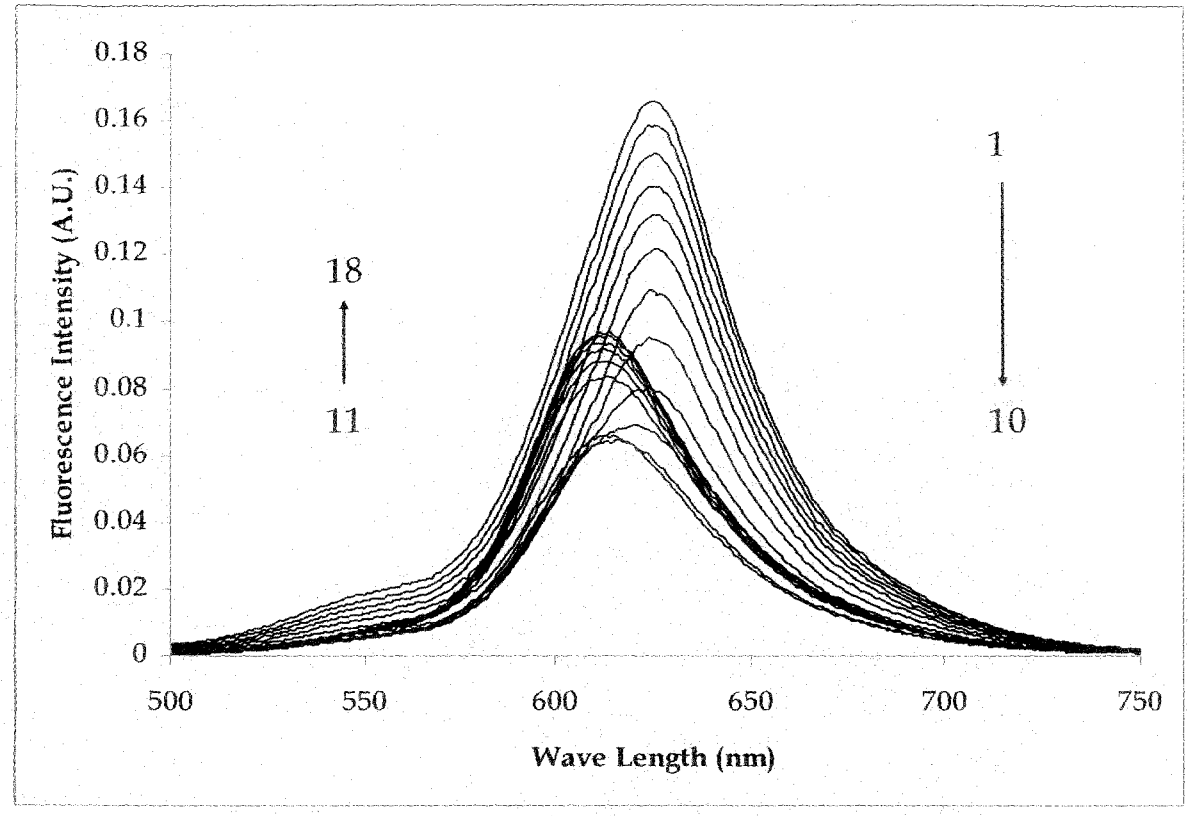

Figure 5.14: Fluorescence spectra of dye in lithium dodecyl benzene sulfonate having concentrations (1) 10 mM (2) 8 mM (3) 6.4 mM (4) 5.12 mM (5) 4.10 mM (6) 3.28 mM (7) 2.62 mM (8) 2.10 mM (9) 1.68 mM (10) 1.34 mM (11) 1.07 mM (12) 0.859 mM (13) 0.687 mM (14) 0.550 mM (15) 0.440 mM (16) 0.352 mM (17) 0.281 mM (18) 0.225 mM at 298 K.

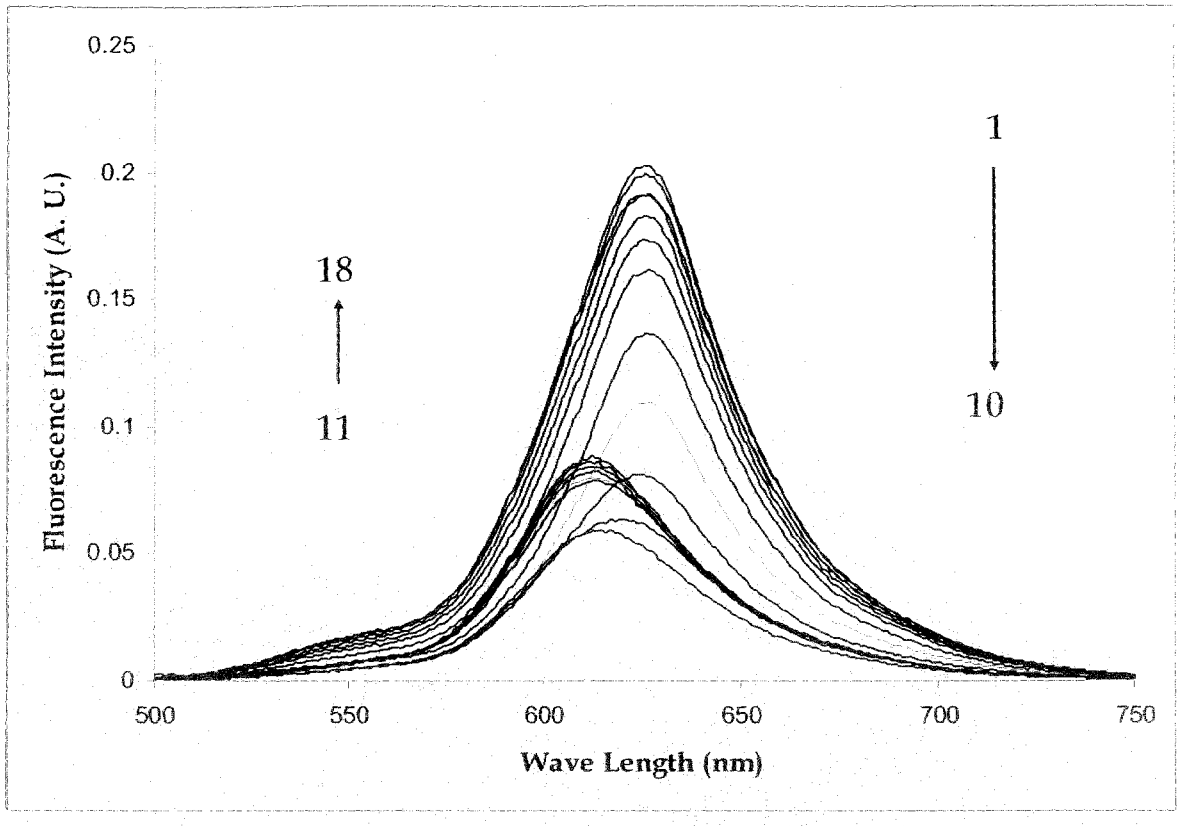

Figure 5.15: Fluorescence spectra of dye in sodium dodecyl benzene sulfonate having concentrations (1) 10 mM (2) 8 mM (3) 6.4 mM (4) 5.12 mM (5) 4.10 mM (6) 3.28 mM (7) 2.62 mM (8) 2.10 mM (9) 1.68 mM (10) 1.34 mM (11) 1.07 mM (12) 0.859 mM (13) 0.687 mM (14) 0.550 mM (15) 0.440 mM (16) 0.352 mM (17) 0.281 mM (18) 0.225 mM at 298 K.

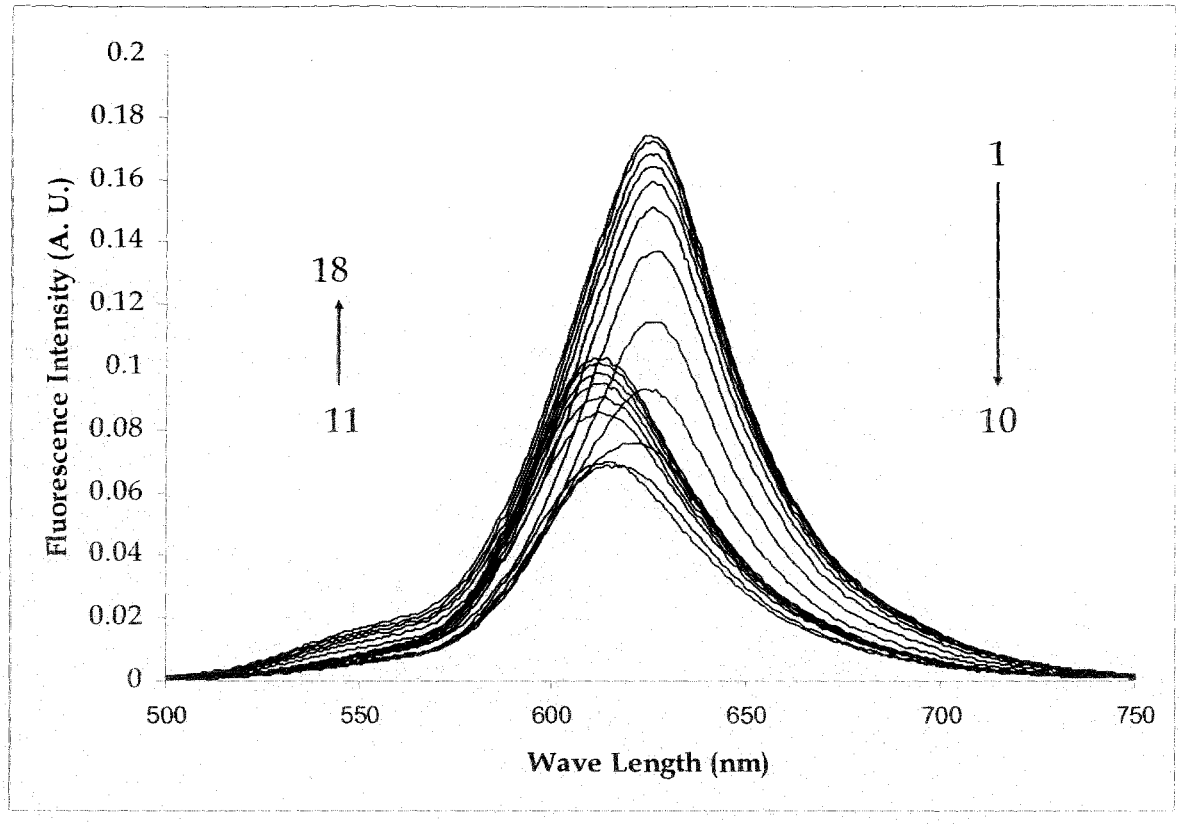

Figure 5.16: Fluorescence spectra of dye in potassium dodecyl benzene sulfonate having concentrations (1) 10 mM (2) 8 mM (3) 6.4 mM (4) 5.12 mM (5) 4.10 mM (6) 3.28 mM (7) 2.62 mM (8) 2.10 mM (9) 1.68 mM (10) 1.34 mM (11) 1.07 mM (12) 0.859 mM (13) 0.687 mM (14) 0.550 mM (15) 0.440 mM (16) 0.352 mM (17) 0.281 mM (18) 0.225 mM at 298 K.

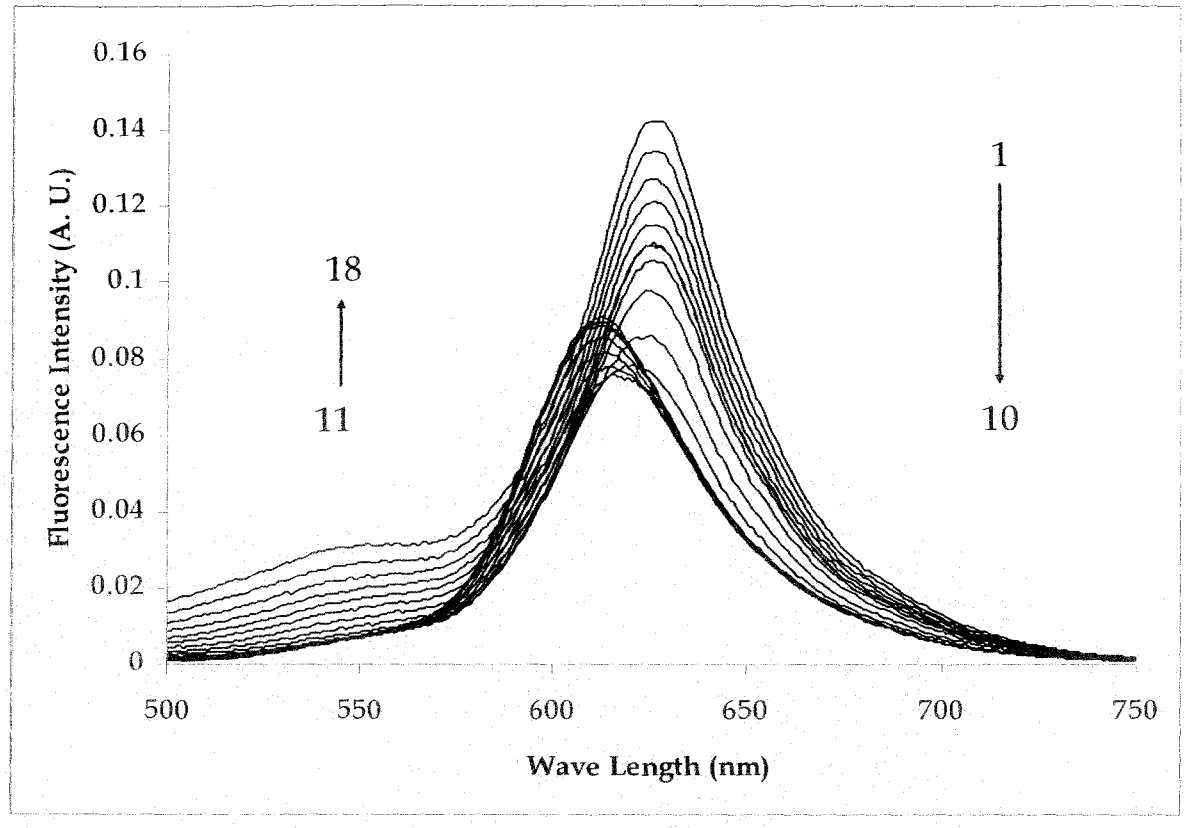

Figure 5.17: Fluorescence spectra of dye in ammonium dodecyl benzene sulfonate having concentrations (1) 10 mM (2) 8 mM (3) 6.4 mM (4) 5.12 mM (5) 4.10 mM (6) 3.28 mM (7) 2.62 mM (8) 2.10 mM (9) 1.68 mM (10) 1.34 mM (11) 1.07 mM (12) 0.859 mM (13) 0.687 mM (14) 0.550 mM (15) 0.440 mM (16) 0.352 mM (17) 0.281 mM (18) 0.225 mM at 298 K.

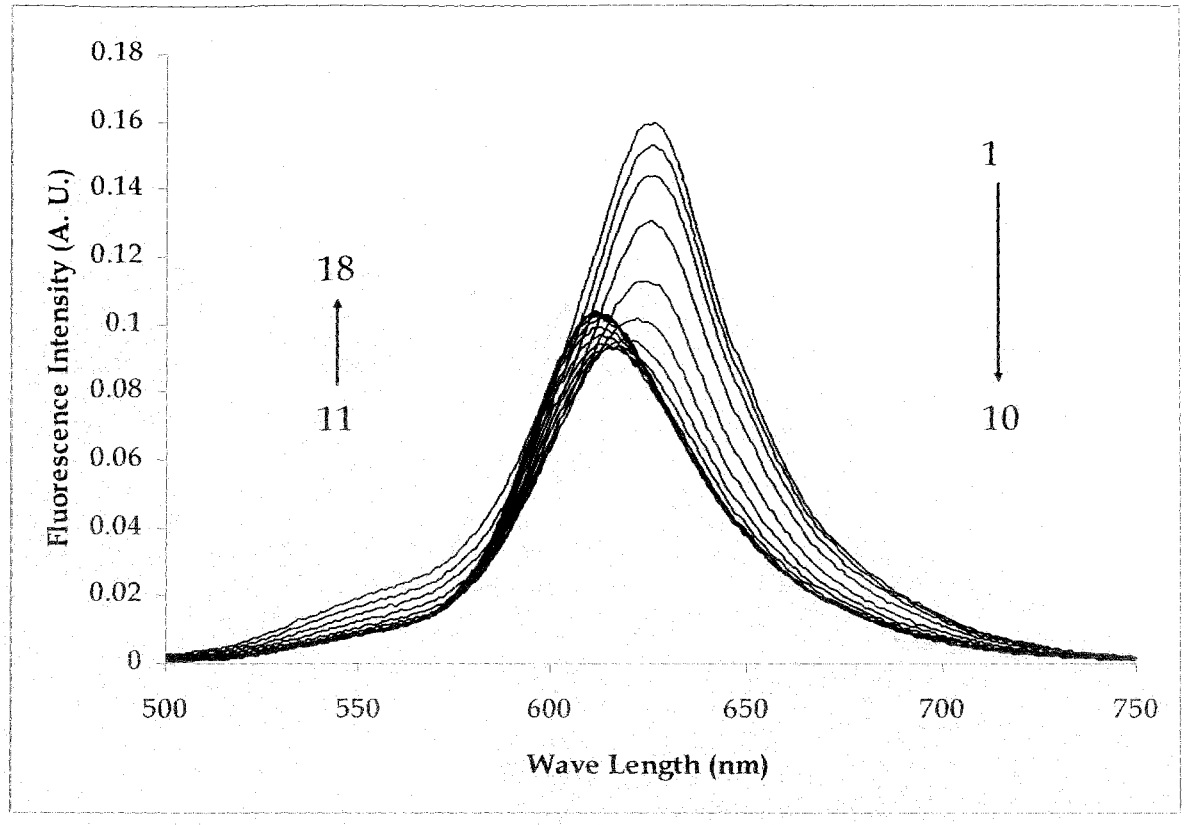

Figure 5.18: Fluorescence spectra of dye in tetramethyl ammonium dodecyl benzene sulfonate having concentrations (1) 10 mM (2) 8 mM (3) 6.4 mM (4) 5.12 mM (5) 4.10 mM (6) 3.28 mM (7) 2.62 mM (8) 2.10 mM (9) 1.68 mM (10) 1.34 mM (11) 1.07 mM (12) 0.859 mM (13) 0.687 mM (14) 0.550 mM (15) 0.440 mM (16) 0.352 mM (17) 0.281 mM (18) 0.225 mM at 298 K.

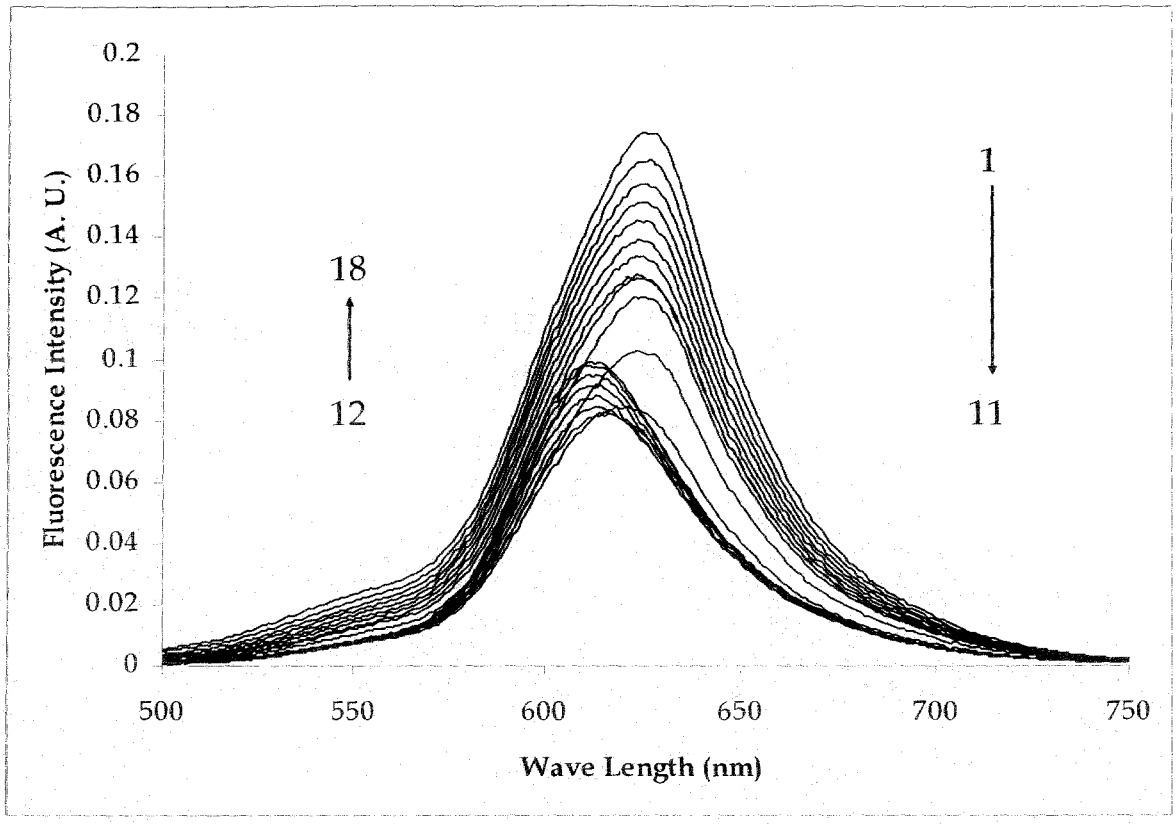

Figure 5.19: Fluorescence spectra of dye in tetraethyl ammonium dodecyl benzene sulfonate having concentrations (1) 10 mM (2) 8 mM (3) 6.4 mM (4) 5.12 mM (5) 4.10 mM (6) 3.28 mM (7) 2.62 mM (8) 2.10 mM (9) 1.68 mM (10) 1.34 mM (11) 1.07 mM (12) 0.859 mM (13) 0.687 mM (14) 0.550 mM (15) 0.440 mM (16) 0.352 mM (17) 0.281 mM (18) 0.225 mM at 298 K.

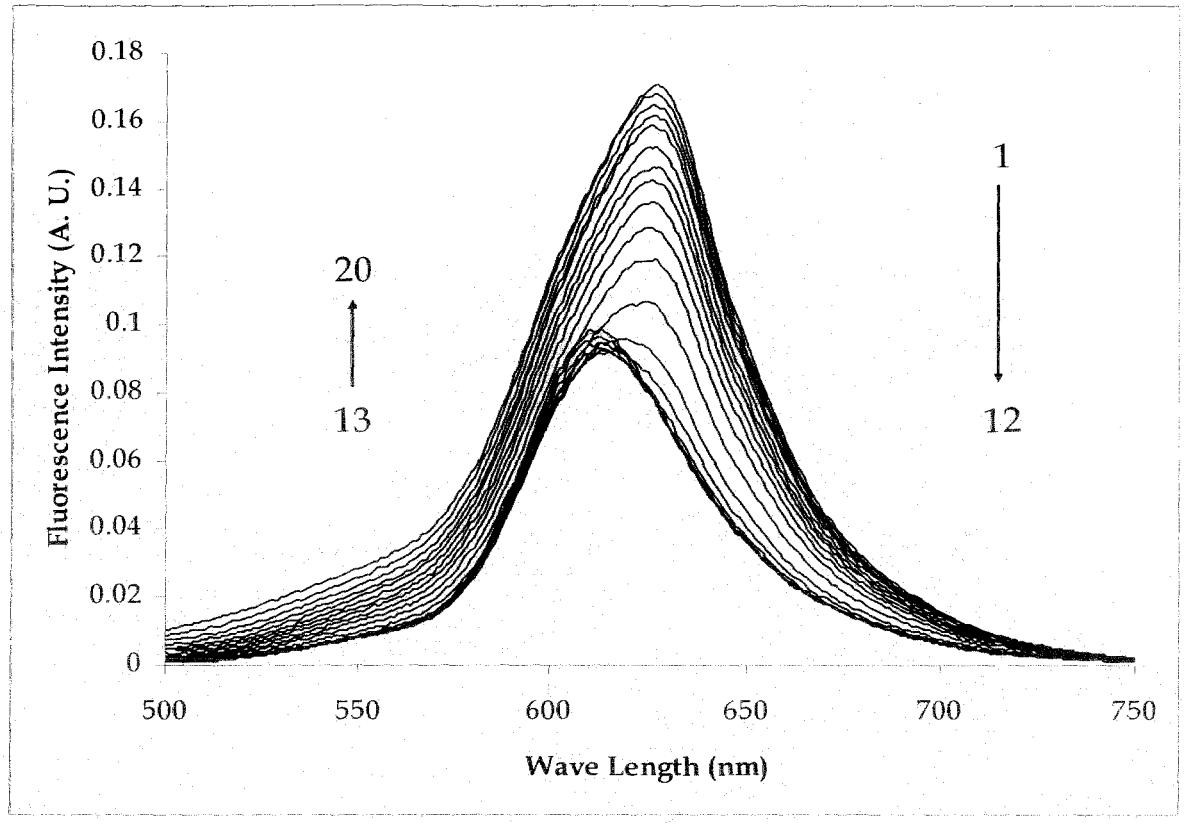

Figure 5.20: Fluorescence spectra of dye in tetrapropyl ammonium dodecyl benzene sulfonate having concentrations (1) 10 mM (2) 8 mM (3) 6.4 mM (4) 5.12 mM (5) 4.10 mM (6) 3.28 mM (7) 2.62 mM (8) 2.10 mM (9) 1.68 mM (10) 1.34 mM (11) 1.07 mM (12) 0.859 mM (13) 0.687 mM (14) 0.550 mM (15) 0.440 mM (16) 0.352 mM (17) 0.281 mM (18) 0.225 mM (19) 0.180 mM (20) 0.144 mM at 298 K.

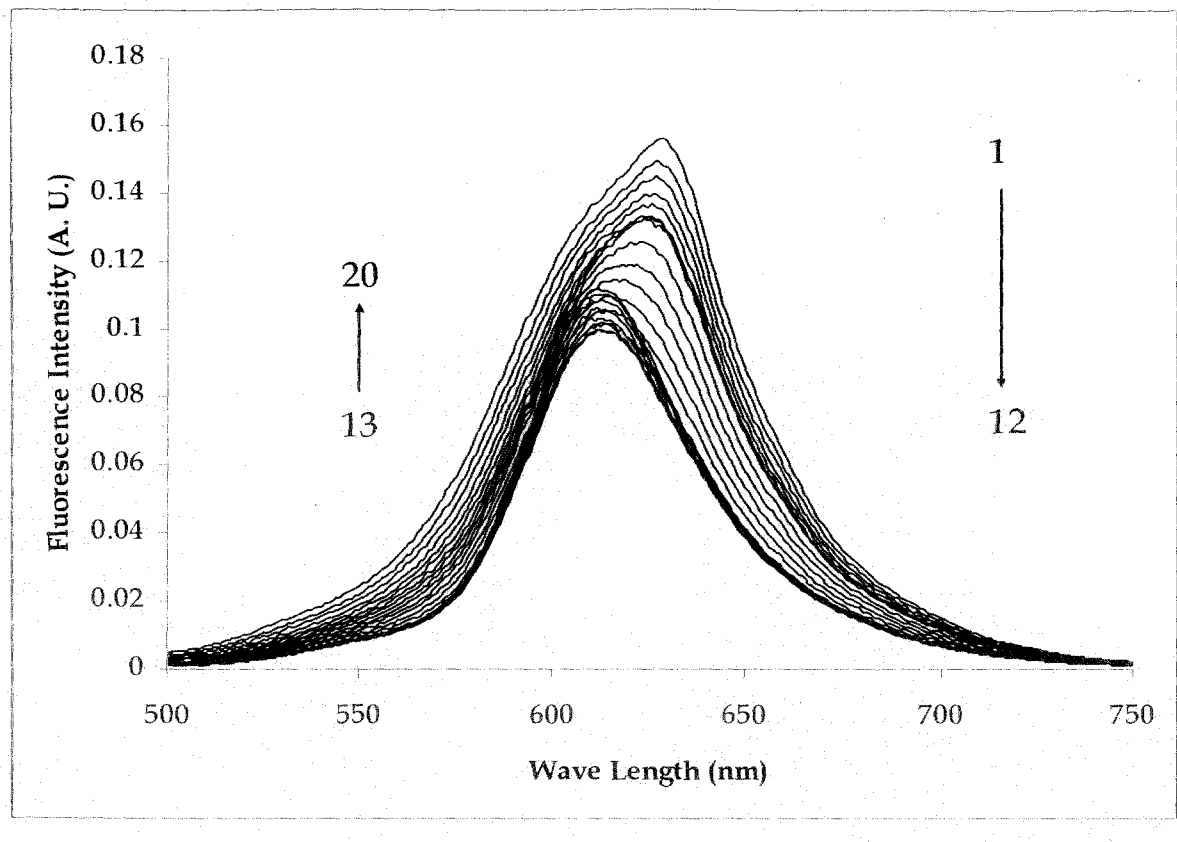

Figure 5.21: Fluorescence spectra of dye in tetrabutyl ammonium dodecyl benzene sulfonate having concentrations (1) 10 mM (2) 8 mM (3) 6.4 mM (4) 5.12 mM (5) 4.10 mM (6) 3.28 mM (7) 2.62 mM (8) 2.10 mM (9) 1.68 mM (10) 1.34 mM (11) 1.07 mM (12) 0.859 mM (13) 0.687 mM (14) 0.550 mM (15) 0.440 mM (16) 0.352 mM (17) 0.281 mM (18) 0.225 mM (19) 0.180 mM (20) 0.144 mM at 298 K.

From all these figures, it can be concluded that at the concentration of the surfactant below cmc, there is also surfactant and dye interaction. With increase in surfactant concentration, fluorescence intensity (A.U.) dropped continuously. After this, the fluorescence intensity increases which show that the monomer is freed from ion-pair or cluster causing increase in fluorescence intensity. The order of the ion pair formation or cluster formation for alkali metal counter ions is as follows: $Li^+ > K^+ > Na^+$ and for tetraalkyl ammonium counter ion along with ammonium ion is as follows: $NH_4^+ > (C_4H_9)_4N^+ > (C_3H_7)_4N^+ > (C_2H_5)_4N^+ > (CH_3)_4N^+$. The counter ion, lithium, has the smallest alkali metal ion with largest hydration sphere causing incorporation of dye into the surfactant. Recent study of this type of complex formation via charge transfer process or electron donor-acceptor complexes was also observed by some researches [60]. The fluorescence intensity of SDBS is greater than LDBS which indicates dye molecules are more free to form the ion-pair or cluster in SDBS due to its

larger size and less attraction. For potassium counter ion, the dye molecules are more free from surfactant compared to lithium but less free from sodium can be explained with increase size of alkali metals and decreasing hydration sphere contributing to the hydrophobic effect for the formation of micelle. The size of the counter ion ammonium is greater than cesium ion but less than tetramethyl ammonium ion which is less free from surfactant compared to all the alkali metal ions due to decreasing hydration sphere contributing to the hydrophobic effect for the formation of micelle. In tetrabutyl ammonium dodecyl benzene sulfonate, the counter ion is tetrabutyl ammonium group which is most hydrophobic in nature as compared to the other groups present. Tetramethylammonium counter ion does not follow the expected trend. The trend can be explained as the consequences of the increased charged screening and higher counter ion binding capacity via stronger hydrophobic interactions with the micelles. In the present study, it is found for all the counter ion that the cmc is lowered which is due to the interactions present between the surfactant and the dye. It is clear that in every case there is a red shift of the peak intensity. This shift is not similar in all the different surfactant because the interaction of the surfactant with the dye is different with change of the counterion. As the counterion gets bulky for the group of tetraalkylammonium ions, the blue shift get increased due to the hydrophobicity present in the group.

To study the quenching of the non-fluorescent aggregates formed with increasing dye concentration, Stern – Volmer (SV) plots were obtained from steady state fluorescence data. Here, the Stern – Volmer equation is

$$\frac{F_0}{F} = 1 + K_{SV}\,[Q] \qquad (5.8)$$

Where F is the fluorescence intensity in presence of quencher; F_0 is the fluorescence intensity in absence of quencher; $[Q]$ is the quencher concentration and K_{SV} is the Stern-Volmer constant, which is equal to $k_q\tau_0$; k_q is the quenching constant and τ_0 is the life time of the fluorophore in absence of quencher. Here, the aggregates are the quenchers. Thus, $[Q] \propto [M]$, where $[M]$ is the monomer concentration [59].

In our present case for all the surfactants, the Stern – Volmer plots deviate from linearity at high dye concentrations. Their upward curvature clearly suggests that both

static quenching and collisional quenching are present here [61]. We have calculated the Stern – Volmer constant for all the surfactants which are given in the table below:

Table 5.3:
Stern-Volmer (K_{SV}) Constants for all the surfactants

Surfactants	K_{SV}/M^{-1}
SDBS	1.90×10^{3}
LDBS	1.30×10^{3}
PDBS	1.04×10^{3}
ADBS	7.53×10^{4}
TMADBS	6.19×10^{4}
TEADBS	5.43×10^{4}
TPADBS	4.36×10^{4}
TBADBS	2.95×10^{4}

A representative plot for sodium dodecyl benzene sulfonate surfactant to calculate stern –volmer constant is given in figure 5.22.

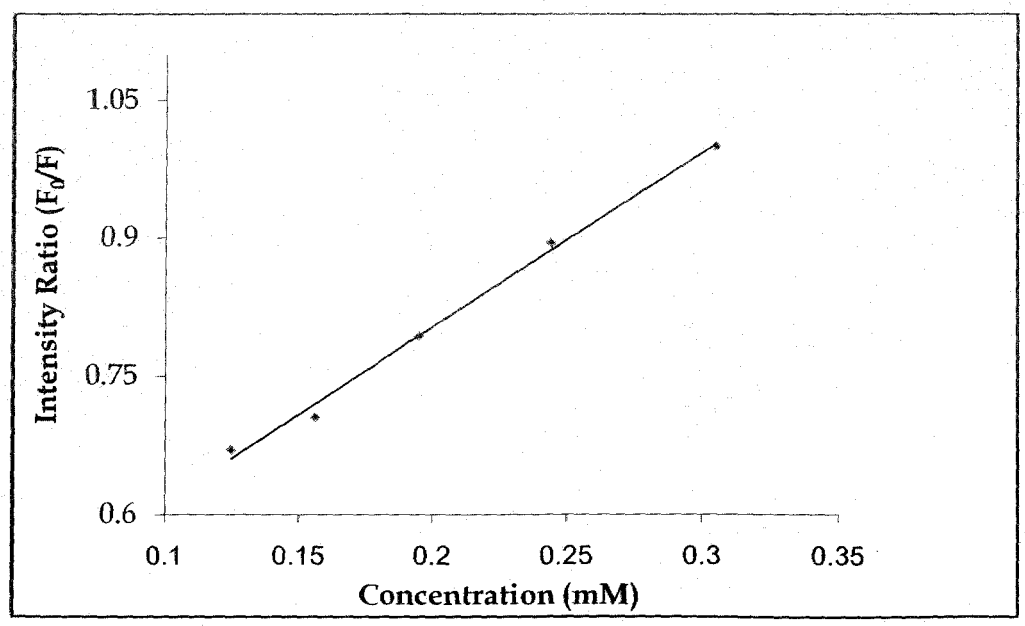

Figure 5.22: Fluorescence intensity ratio vs. concentration (mM) of sodium dodecyl benzene sulfonate surfactant.

Here, from the Stern - Volmer constant values we see that most of the constants are of the same order. However, a closer look at the Stern-Volmer constant values, which are

the measure of the extent of the interaction of dye in the excited states with the surfactant at sub-micellar concentrations, show that such interaction is almost same for all the inorganic counter ions. For the organic counter ions, on the other hand, extent of interaction decreases as the size of the counter ion increases. Therefore, quenching of dye fluorescence due to collision and energy transfer by either the monomer or the dimer is possible though there is some discrepancies which may be due to the size and hydrophobicity of the counterion present with the dodecyl benzene sulfonate moiety.

5.5 Anisotropy

5.5.1. Theory of anisotropy

Anisotropy measurements are commonly used in the bio-chemical application of fluorescence. Anisotropy measurements provide information on the size and shape of proteins or the rigidity of various molecular environments. Anisotropy measurements have been used to measure protein-protein associations and fluidity of membranes and for immunoassays of numerous substances. Anisotropy measurements are based on the principle of photoselective excitation of fluorophores by polarized light. Fluorophores preferentially absorb protons whose electric vectors are aligned parallel to the transition moment of the fluorophore. The transition moment has a defined orientation with respect to the molecular axes. In an isotropic solution, the fluorophores are oriented randomly. Upon excitation with polarized light, one selectively excites those fluorophore molecules whose absorption transition dipole is parallel to the electric vector of the excitation. This selective excitation results in a partially oriented population of fluorophores (photoselection) and in partially polarized fluorescence emission. Emission also occurs with the light polarized along a fixed axis in the fluorophore. The relative angle between these moments determines the maximum measured anisotropy. The fluorescence anisotropy (r) and polarization (P) are defined by

$$r = \frac{I_{\parallel} - I_{\perp}}{I_{\parallel} - 2\,I_{\perp}} \qquad (5.9)$$

$$P = \frac{I_{\parallel} - I_{\perp}}{I_{\parallel} + I_{\perp}} \qquad (5.10)$$

where $I_{\parallel}$ and $I_{\perp}$ are the fluorescence intensities of the vertically and horizontally polarized emission, when the sample is excited with vertically polarized light. That is anisotropy is the absorption of light by a fluorophore along a particular direction with respect to the molecular axes.

In the present experiment, the oxazine dye with dodecyl benzene sulfonate with varying counter ions has been used. As discussed in the previous part, the oxazine dyes display surprising long-wavelength absorption and emission maxima in fluorescence which makes these groups of dye an important fluorescent probe. We have studied the anisotropy measurements of surfactants by Cresyl fast violet (CFV).

5.5.2 Materials and methods

Materials

As discussed in the previous part of this chapter.

Methods

Anisotropy measurement was done with the same Fluorosence Spectrophotometer, Photon Technology Inc. Co., USA. In all the experiment, the concentration of the dye is very low, 1×10^{-6} (M). Quartz cuvettes were employed throughout the measurements of anisotropy measurements. The data were analyzed with the software given "Felix GX" with the instruments to get the polarization values.

5.5.3 Results and discussions

The anisotropy/polarization data of surfactant-cresyl fast violet solution derived by the software 'Felix GX', supplied by the manufacturer with the fluorescence spectrophotometer instrument, as a function of surfactant concentration are shown in Table 5.4.

Table 5.4.
Polarization value for fluorescence emission of cresyl fast violet in presence of surfactant with different counterions at 298 K

[Surfactant] mM	Polarisation values due to different counter ions							
	Na^+	Li^+	K^+	NH_4^+	TMA^+	TEA^+	TPA^+	TBA^+
10.00	0.1274	0.1328	0.1366	0.1347	0.1632	0.1429	0.1606	0.1961
8.000	0.1249	0.1299	0.1320	0.1309	0.1608	0.1426	0.1577	0.1876
6.400	0.1185	0.1280	0.1280	0.1299	0.1608	0.1407	0.1552	0.1804
5.120	0.1177	0.1265	0.1256	0.1292	0.1600	0.1394	0.1533	0.1745
4.100	0.1195	0.1250	0.1219	0.1271	0.1577	0.1384	0.1527	0.1697
3.280	0.1174	0.1162	0.1189	0.1247	0.1539	0.1385	0.1514	0.1665
2.620	0.1141	0.1050	0.1097	0.1222	0.1496	0.1379	0.1502	0.1634
2.100	0.1105	0.1000	0.1045	0.1197	0.1341	0.1380	0.1500	0.1607
1.680	0.1048	0.0960	0.0961	0.1120	0.1229	0.1350	0.1483	0.1579
1.340	0.0955	0.1059	0.0960	0.1052	0.1136	0.1278	0.1459	0.1545
1.070	0.0855	0.1138	0.1145	0.1084	0.1248	0.1235	0.1436	0.1497
0.859	0.0939	0.1101	0.1120	0.1159	0.1360	0.1116	0.1382	0.1462
0.687	0.1019	0.1068	0.0989	0.1049	0.1248	0.1044	0.1258	0.1399
0.550	0.1081	0.1052	0.0910	0.1186	0.1197	0.1091	0.1208	0.1350
0.440	0.1012	0.1034	0.0939	0.1089	0.1040	0.1182	0.1089	0.1269
0.352	0.0928	0.1014	0.0945	0.1096	0.0789	0.1000	0.0929	0.1336

The steady-state anisotropy or polarized fluorescence study provides a simple way of monitoring any process where the microstructure is affected in some way [62]. Further, the anisotropy is considered as an index of the micro-viscosity or rigidity in the microenvironment of the probe [63]. The polarization values from steady-state anisotropy underline the effect of hydration on the microstructure of micelle or dye – surfactant complex [64]. Actually, the degree of depolarization of the fluorescence emission of a molecular probe is a measure of its rotational diffusion during the excited life time [65-66]. So, fluorescence anisotropy (r) is an experimental measurement of the fluorescence. The lower the anisotropy value, the faster is the rotational diffusion [62]. Polarization values for the surfactant dodecyl benzene sulfonate with varying counter ions are given in the table 5.4. The trend is normal for all the surfactant except lithium dodecyl benzene sulfonate and ammonium dodecyl benzene sulfonate due to high hydration enthalpy of lithium and intermediate size of the ammonium ion.

From table 5.4, it is also clear that at high surfactant concentration, the rotational diffusion of the probe is restrained. Consequently, the probe does not assume all possible orientations with equal probability [67]. In all the surfactant, the anisotropy value (r) gradually decreases upto the micelle formation stage and then increases. The interpretation of the results also emerges from steady-state anisotropy of these dye-surfactant complex system is not straightforward; its value depends on various factors such as, the rotational motion and the possible dye - surfactant interactions. A plausible explanation for the decrease in polarization value with decrease in surfactant concentration is that at high surfactant concentration, the micelle hinders the rotation of the dye molecule in solution [67]. But with decease in surfactant concentration, the packing of amphiphiles at the interface is less compact which show a decrease in polarization value. Below the cmc, the increase in polarization value can also attributed to the higher dye-surfactant interactions.

Table 5.5.
Table for concentration break points by polarization values.

Surfactants	Concentration at break points (M)	Polarisation Value at break points
SDBS	2.362×10^{-3}	0.1144
LDBS	3.015×10^{-3}	0.1189
KDBS	2.912×10^{-3}	0.1195
ADBS	2.310×10^{-3}	0.1423
TMADBS	2.810×10^{-3}	0.1524
TEADBS	1.620×10^{-3}	0.1362
TPADBS	0.825×10^{-3}	0.1475
TBADBS	1.120×10^{-3}	0.1560

The anisotropy of the cresyl fast violet increases gradually for all the surfactant and it levels off at the value of 1×10^{-2} (M) concentration of the surfactant. The observed changes in anisotropy of cresyl fast violet as function of surfactant concentration also provide evidence of different types of interactions above and below the cmc. Upon addition of surfactant, the anisotropy initially increases fast, but this increase in a range of very low surfactant concentration and below the cmc. This is the evidence of interactions that reduce the dye's ability to rotate freely. A dye-surfactant ionic pair or cluster would result in such a decreased ability to rotate because of its larger size than an individual dye ion. The increase polarization value with increasing surfactant concentration probably means that more surfactant molecule join the clusters as the

surfactant concentration increases. Around the cmc, the increase of anisotropy value drops to an extent. This point may be a caused by the surfactant forming micelles preferentially to ionic interactions with the dye. This could free up some of the dye molecule from their ionic interactions with the surfactant monomers. Above the cmc, the anisotropy increases to a very little before leveling off at two or three times the anisotropy of cresyl fast violet. This shows that the dye is less free to rotate in the miceller environment. Micelles contain a large number of surfactant monomers, so they rotate slowly. A dye molecule trapped within such a micelle would also rotate slowly, causing a high anisotropy. The dye's lower ability to rotate above the cmc shows that it is within the micelle in a more rigid formation. This may be because the positively charged end of the dye is interacting with the negatively charged ends of the surfactant ions. The value of the cmc derived from polarization value is in good agreement with the value determined by surface tension and conductometically for each of the surfactant. The slight difference between two is due to the two other methods applied to explain the facts and also dye surfactant interactions present in the latter system, with only exception in tetrabutyl ammonium dodecyl benzene sulfonate. For the case of TBADBS surfactant, apart from hydrophobic effect the alkyl chain length is also a predominating factor for its properties. Due to its chain length, hydrophobicity increases, and as a result the dye surfactant interactions increases, and so the cmc increases. The plots for polarization values vs. concentration plots for all the surfactants are given in below (figure 5.23 – 5.30).

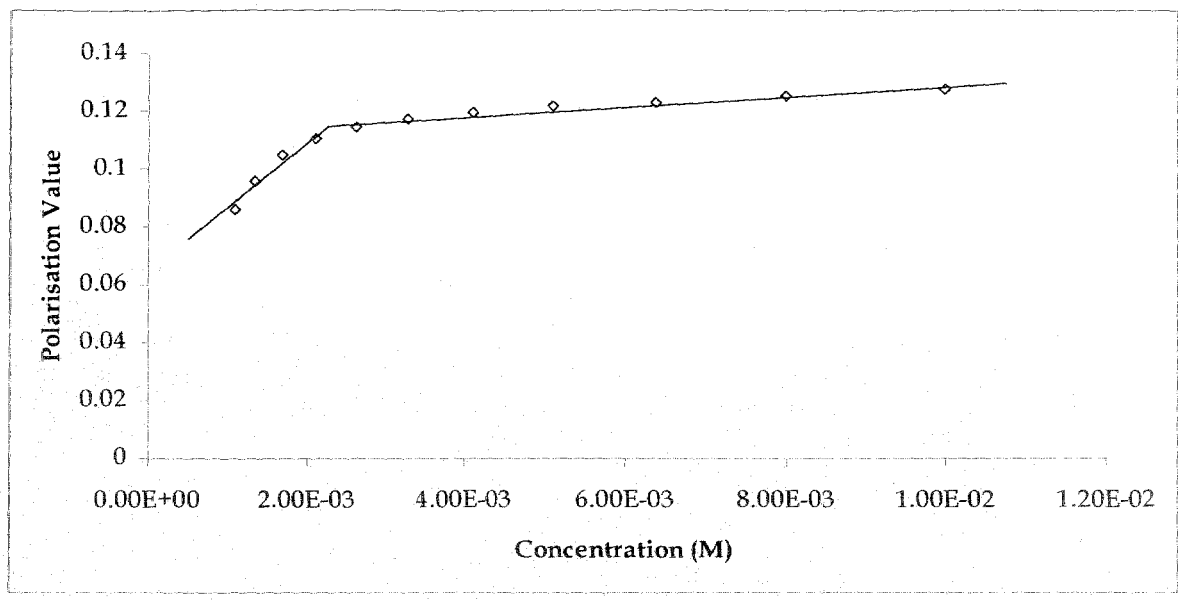

Figure 5.23: Polarisation value vs. concentration of the surfactant plot of sodium dodecyl benzene sulfonate

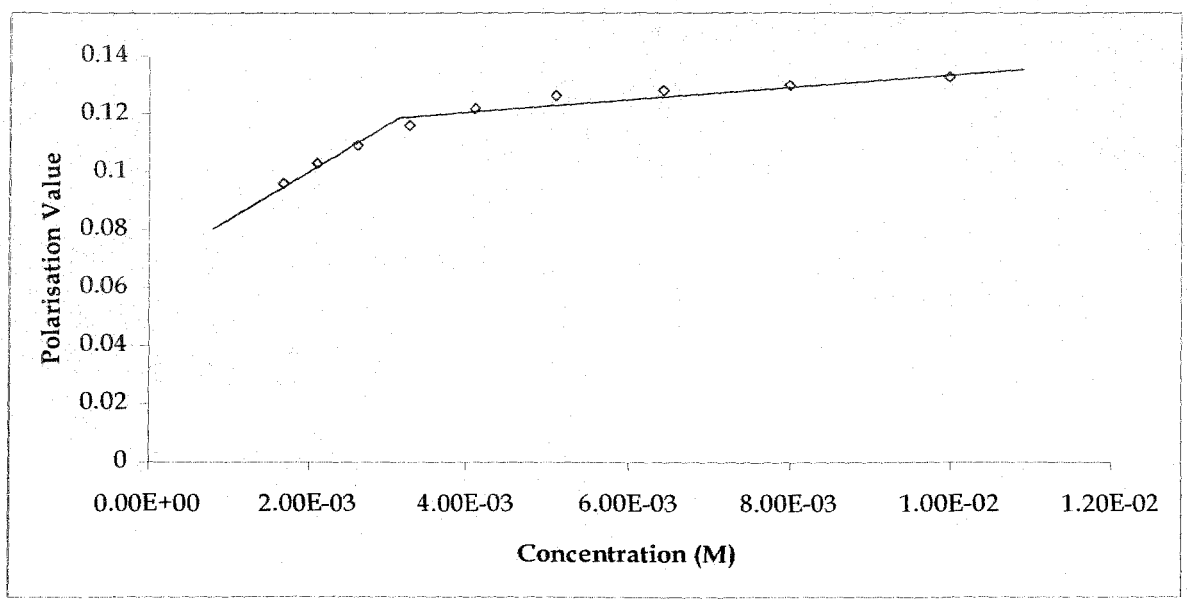

Figure 5.24: Polarisation value vs. concentration of the surfactant plot of lithium dodecyl benzene sulfonate

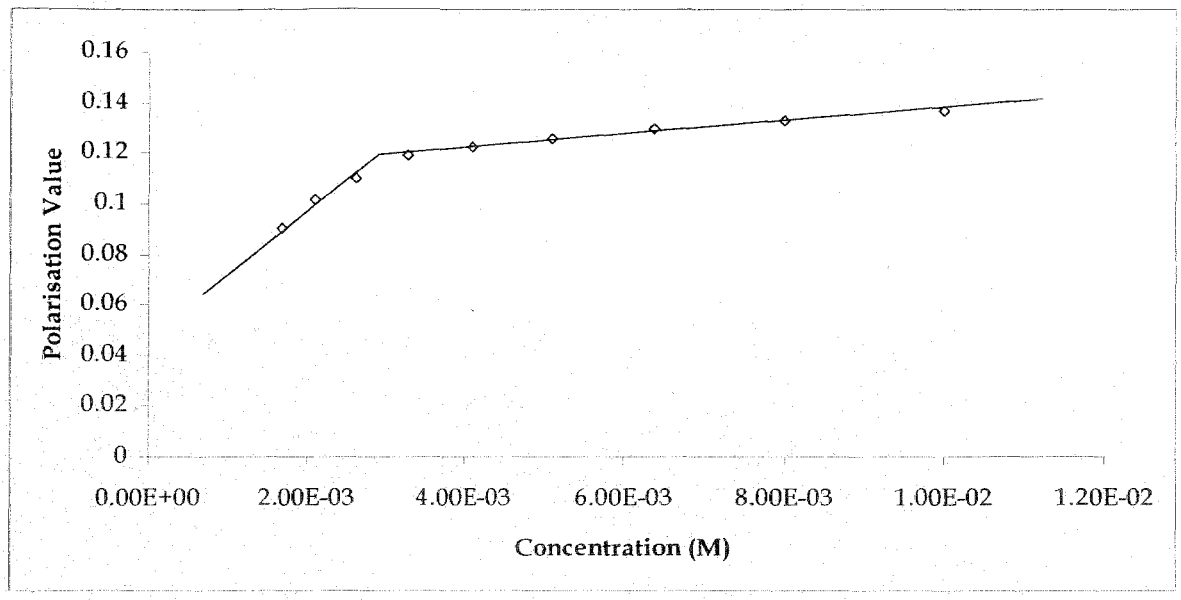

Figure 5.25: Polarization value vs. concentration of the surfactant plot of potassium dodecyl benzene sulfonate.

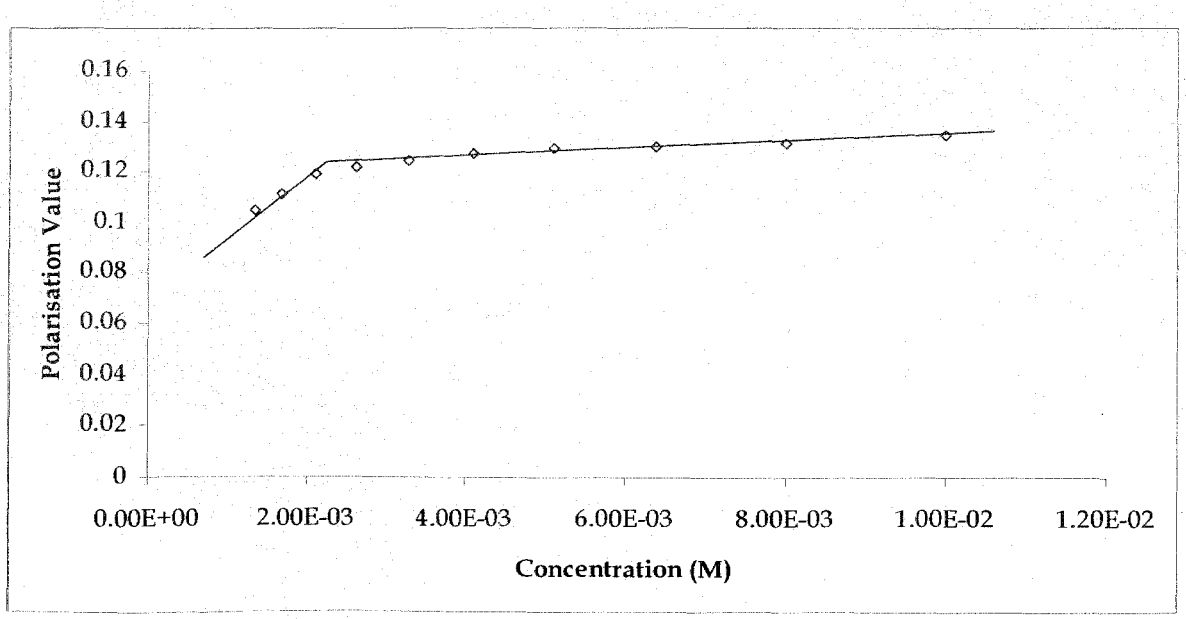

Figure 5.26: Polarization value vs. concentration of the surfactant plot of ammonium dodecyl benzene sulfonate.

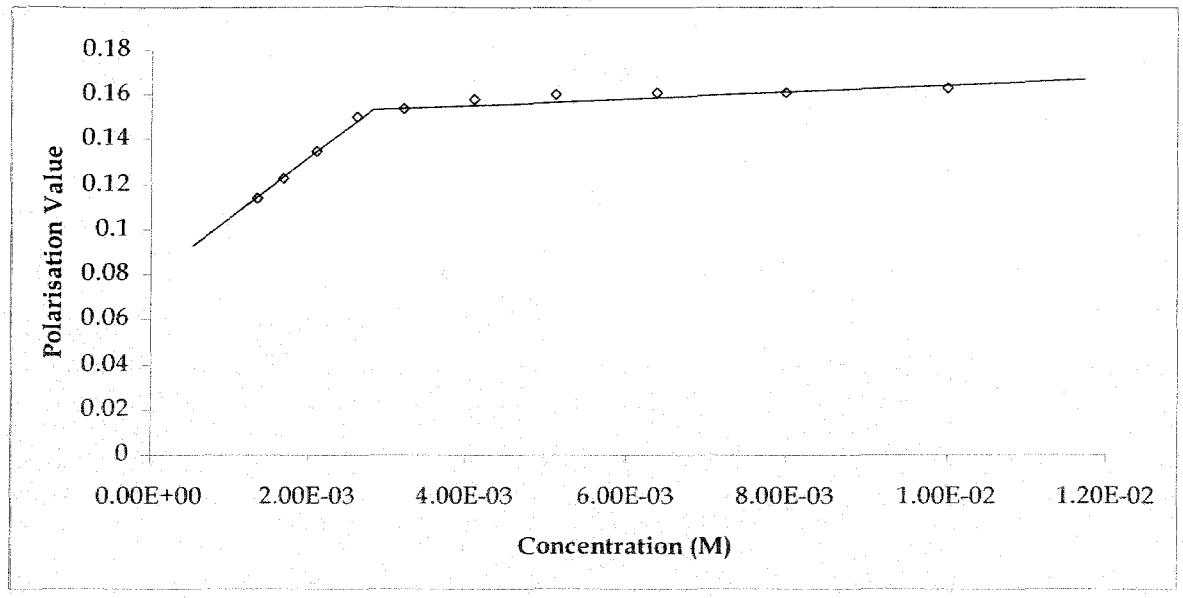

Figure 5.27: Polarization value vs. concentration of the surfactant plot of tetramethyl ammonium dodecyl benzene sulfonate.

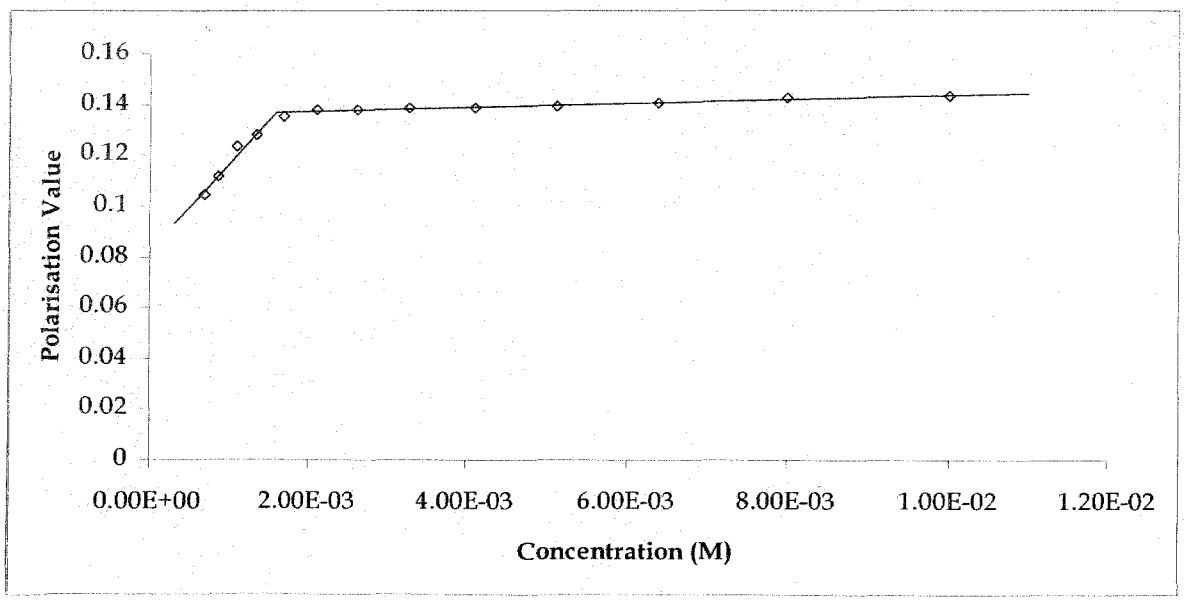

Figure 5.28: Polarisation value vs. concentration of the surfactant plot of tetraethyl ammonium dodecyl benzene sulfonate.

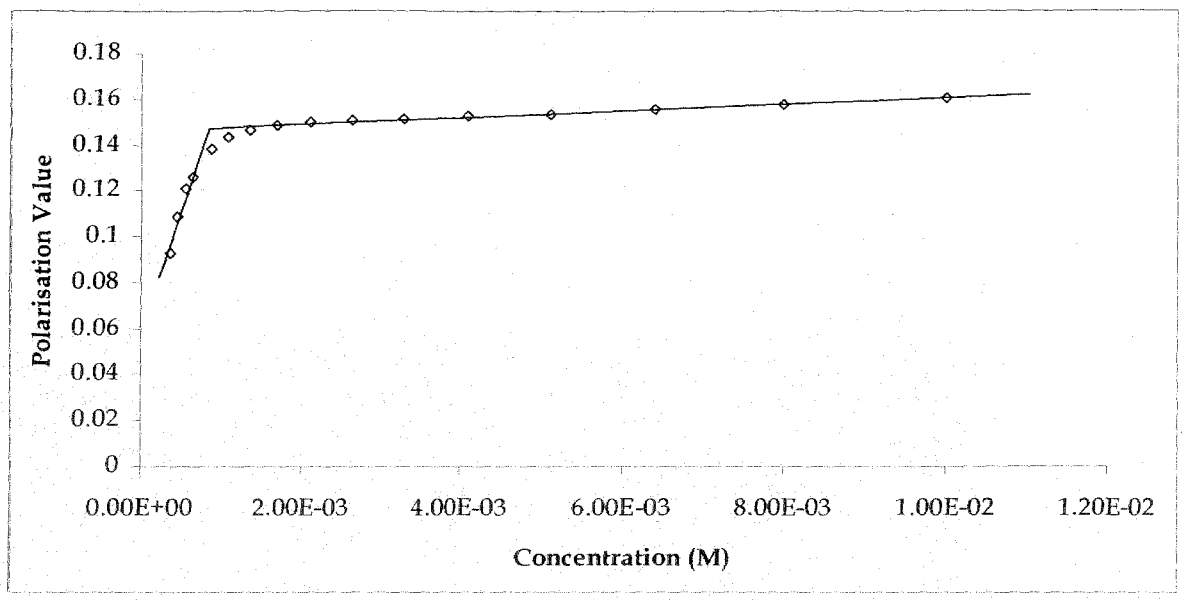

Figure 5.29: Polarisation value vs. concentration of the surfactant plot of tetrapropyl ammonium dodecyl benzene sulfonate.

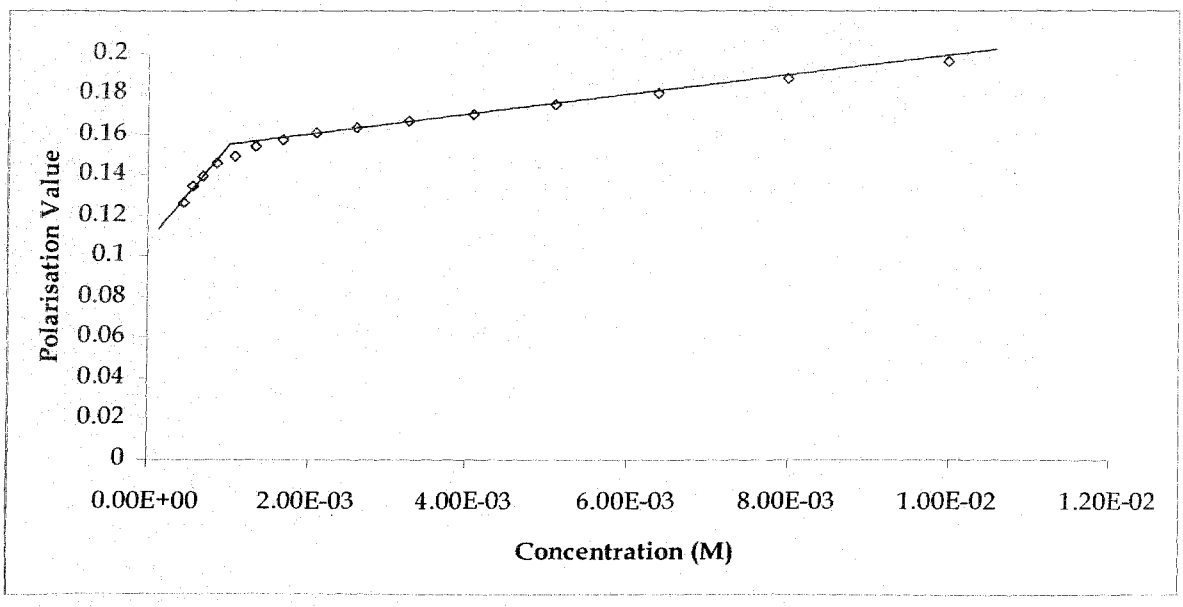

Figure 5.30: Polarisation value vs. concentration of the surfactant plot of tetrabutyl ammonium dodecyl benzene sulfonate.

5. 6. Lifetime measurements

Time-resolved measurements are widely used in fluorescence spectroscopy, particularly for studies of biological macromolecules. This is because time-resolved data frequently contain more information than is available from steady-state data. Two methods of measuring time-resolved fluorescence are in widespread use, the time-domain and frequency-domain methods. In time-domain or pulse fluorometry, the sample is excited with a pulse of light. The width of the pulse is made as short as possible and is preferably much shorter than the decay time τ of the sample. The time-dependent intensity is measured following the excitation pulse, and the decay time τ is calculated from the slope of a plot of log I(t) versus t, or from the time at which the intensity decreases to 1/e of the value at t = 0. The intensity decays are often measured through a polarizer oriented at 54.7° from the vertical z-axis [28].

In the present experiment, time resolved fluorescence studies were carried out to determine the emission decay parameters of all the surfactants with different surfactant concentrations. The concentration of the dye used was 5×10^{-6} (M). As a nanosecond set up was used, very fast decay could not be recorded. Thus, high dye concentrations could not be used, as at these concentrations lifetime values may be drastically decreased due to fluorescence quenching. Another experimental restriction is that, the 0.5 cm path length cell could not be inserted into the cell holder for lifetime studies. With a cell of larger path length, inner filter effects interfere with the fluorescence studies for very concentrated solutions [52,61]. So, only four set of concentrations for each dye have been taken for study and the values are given on the table 5.6. The lifetime values did not change significantly or in a regular manner with the change in surfactant concentration suggesting single exponential fluorescence decay curve for all the surfactants.

Table5.6.
Life time for all the surfactant with varying counter ions

Surfactant/ Concentration	0.01M	0.005M	0.0005M	0.0001M
LDBS	2.9 ns	3.0 ns	2.9 ns	2.5 ns
SDBS	3.2 ns	3.6 ns	3.5 ns	1.5 ns
KDBS	3.4 ns	3.3 ns	1.9 ns	4.3 ns
NH_4DBS	2.9 ns	3.3 ns	2.5 ns	2.9 ns
TMADBS	4.4 ns	2.5 ns	3.4 ns	4.9 ns
TEADBS	3.8 ns	2. 8 ns	3.3 ns	2.5 ns
TPADBS	3.5 ns	4.8 ns	3.7 ns	2.4 ns
TBADBS	4.3 ns	2.6 ns	2.5 ns	2.2 ns

References:

1. Tanford, C. *'The Hydrophobic Effect: Formation of Micelles and Biological Membranes"*, Wiley, New York, N. Y., 1973.

2. Kalyanasundaram, K.; Thomas, J. K. *J. Am. Chem. Soc.* **1977**, 99, 2039-2044.

3. Kalyanasundaram, K.; Thomas, J. K. *J.Phys. Chem.* **1977**, 81, 2176-2180.

4. Turro, N. J.; Okubo, T. *J. Phys. Chem.* **1982**, 86, 159-161.

5. Turro, N. J.; Okubo, T. *J. Am. Chem. Soc.* **1981**, 103, 7224-7230.

6. Levitz, P.; Van Damme, H.; Keravis, D. *J. Phys. Chem.***1984**, 88, 2228-2235.

7. Turro, N. J.; Pierola, I. F.; *Macromolecules* **1983**, 16, 906-910.

8. Turro, N. J.; Baretz, B. H.; Kuo, P. C.; *Macromolecules*, **1984**, 17, 1321-1324.

9. Ananthapadmanabhan, K. P.; Leung, P. S.; Goddard, E. D. *Colloids Surf.* **1985**, 13, 63-72.

10. Zana, R.; Yiv, S.; Strazielle, C.; Lianos, P. *J. Coll. Interface Sci.* **1981**, 80, 208-232.

11. Rosen, M. J. *Surfactants and Interfacial Phenomena*; John Wiley: New York, **1989**.

12. Mizusaki, M.; Morishima, Y.; Dubin, P. L. *J. Phys. Chem. B* **1998**, 102, 1908.

13. Zana, R.; Ed.; M. Dekker Inc.: *Surfactant Solution. New Methods of Investigation.*Newyork, **1987**.

14. Cabane, B. In ref 12, Chapter 2, p 57

15. Zana, R.; Ed.; M. Dekker Inc.: *Surfactant Solution. New Methods of Investigation.*Newyork, **1987**.

16. Zana, R. In ref 12; Chapter 5 and references therein.

17. Almgren, M. *Adv. Colloid Interface Sci.* **1992**, 41, 9

18. Gehlen, M.; De Schryver, F. C. *Chem. Rev.* **1993**, 93, 199.

19. Barzykin, A. V.; Tachiya, M. *Heterog. Chem. Rev.* **1996**, 3, 105.

20. Infelta, P. *Chem. Phys. Lett.* **1979**, 61, 88

21. Yekta, A.; Aikawa, M.; Turro, N. *Chem. Phys. Lett.* **1979**, 63, 543.

22. Valeur, B.; Berberan-Santos, M. N. *J. Chem. Educ.*, 2011, 88 (6), 731 – 738.

23. Anathapadmanabhan, K. P.; Goddard, E. D.; Turro, N. J.; Kuo, P. L. *Langmuir* **1985**, 1, 352-355.

24. E. Rodenas and E. Perez-Benito, *J. Phys. Chem*, **1991**, 95, 4552-4556.

25. Hait, S.K.; Majhi, P. R.; Blume, A. and Moulik, S. P., *J. Phys. Chem. B*, **2003**, 107, 3650-3658.

26. Chakraborty, A.; Saha, S. K. and Chakraborty, S. *Colloid Polym. Sci.*, **2008**, 286, 927-934.

27. Benrraou, M.; Bales, B. L. and Zana, R., *J. Phys. Chem. B*, **2003**, 107, 13432-13440.

28. Lakowicz, J. R., *Principles of Fluorescence Spectroscopy*, Plenum Publishers, 2nd Edition, **1999**,

29. Singhal, G. S., Rabinowich, E., and Hevesi, J.*Photochem. Photobiol.* **1970**, 11, 530.

30. Kundu, K.; Bardhan, S.; Banerjee, S.; Chakraborty, G.; Saha, S. K.; Paul, B. K., *Colloid and Surf.*, **2015**, 469, 117 - 131.

31. Snavely, in: J. B. Birks (Ed.), *Organic molecular photophysics*, Wiley, New York, **1973.**

32. Valdes-Aguilera, O.; Necbees, *Acc. Chem. Res.* **1989**, 22, 171 - 177.

33. Lopez Arbeloa, I., P. Ruiz Ojeda, P. *Chem. Phys. Lett.* **1982**, 87, 556.

34. Lopez Arbeloa, I., Rohatgi Mukherjee, K. K., *Chem. Phys. Lett.*, **1986**, 128, 474.

35. Lopez Arbeloa, I., Gonzalez, I. L., Ojeda, P. R.; Lopez Arbeloa, N., *J. Chem. Soc. Faraday Trans.* 2, **1982**, 78, 989.

36. Lopez Arbeloa, I., *Dyes and Pigmets,1983*, 4, 213.

37. Lopez Arbeloa, I., An. Quim. **1984**, 80, 7.

38. Lopez Arbeloa, I., *JCS Faraday Trans.*2, **1981**, 77, 1725 - 1735.

39. Rohatgi, K. K., Mukhopadhay, A. K., *Chem, Phys. Lett.* **1971**, 12, 259.

40. Rohatgi, K. K., Mukhopadhay, A. K., *J. Phys.Chem.* **1972**, 76, 3970.

41. Kamat, P. V., Karkhanavala, M. D., and Moorthy, P. N., *Indian J. Chem. A*, **1977**, 15, 342.

42. Kamat, P. V., Karkhanavala, M. D., and Moorthy, P. N., *Solar Energy*, **1978**, 20, 171.

43. Liu, D., and Kamat, P. V., *J. Chem. Phys.*, **1996**, 105, 965.

44. Martini, I., Hartland, G. V., and Kamat, P. V., *J. Phys. Chem. B*, **1997**, 101, 4826.

45. Anfinrud, P., Crackel, R. L., and Struve, W. S., *J. Phys. Chem.*, **1984**, 88, 5873.

46. Liu, D., Fessenden, R. W., Hug, G., and Kamat, P. V., *J. Phys. Chem. B*, **1997**, 101, 2583.

47. Liu, D., and Kamat, P. V., *Langmuir*, **1996**, 12, 2190.

48. Dutta, R. K., and Bhat, S. N., *Bull. Chem. Soc. Jpn.*, **1992**, 65, 1089.

49. Dutta, R. K., and Bhat, S. N., *Colloids Surf. A*, **1996**, 106, 127.

50. Shah, S. S., Ahmad, R., Shah, S. W. H., Asif, K. M., and Naeem, K., *Colloids Surf. A*, **1998**, 137, 301.

51. Chibisov, A. K., Prokhorenko, V. I., and Gomer, H., *Chem. Phys.*, **1999**, 250, 47.

52. Gawandi, V. B.; Guha, S. N., Priyadarsini, K. I. and Mohan, H. *J Colloid and Interface Science*, **2001**, 242, 220 – 229.

53. Herschel, Sir J. F. W., 1845, *Phil. Trans.* R. Soc. London 135: 143 - 145

54. Rahavendran, S. V., Karnes, H. T., **1996**, *J. Pharm. Biomed. Anal.* 15: 83-98.

55. Flanagan, J. H.; Romeo, S. E.; Legendre, B. L.; Hammer, R. P.; Soper, A.; **1997**, *SPIE*, 2980: 328-337.

56. Selwyn, J. E.; Steinfeld, J. I.; *J. Phys. Chem.* **1972**, 76: 762.

57. Hinckly, D. A.; Seybold, P. G.; Borris, D. P.; *Spectrochim. Acta. A.* **1986**, 42, 747.

58. Chakraborty, M.; Panda, A. K., *Spectrochimica Acta Part A*, **2011**, 81, 458 – 465.

59. De, S.; Das, S.; Girigoswami, A.; *Spectrochimica Acta Part A*, **2005**, 61, 1821 – 1833.

60. R. Adhikari, *Ph.D. Thesis*, **2004**.

61. Lakowicz, J. R. *Principles of fluorescence Spectroscopy*, Kluwer, **1999**, Ch. 8

62. Paul, S.; Panda, A. K., *Colloids Surf. A*, **2013**, 419, 113-124.

63. Jana, B.; Ghosh, S.; Chattapadhaya, N*J. Photochem. Photobiol. B*, **2013**, 126, 1 – 10.

64. Wittouck, N., Negri, R. M., Ameloot, M., De Schryver, F. C., *J. Am. Chem. Soc*, **1994**, 116, 10601-10611.

65. Bardhan, S., Kundu, K., Saha, S. K., Paul, B. K., *Colloids Surf. A*, **2014**, 450, 130 – 140.

66. Ruiz, C. C., Aguiar, J., *Langmuir*, **2000**, 16, 7946 – 7953.

67. Valeur, B., Keh, E., *J. Phys. Chem. B.* **1979**, 83, 3305 – 3307.